

Contents lists available at ScienceDirect

# Palaeogeography, Palaeoclimatology, Palaeoecology

journal homepage: www.elsevier.com/locate/palaeo



# The late quaternary tectonic, biogeochemical, and environmental evolution of ferruginous Lake Towuti, Indonesia



James M. Russell<sup>a,\*</sup>, Hendrik Vogel<sup>b</sup>, Satria Bijaksana<sup>c</sup>, Martin Melles<sup>d</sup>, Alan Deino<sup>e</sup>, Abdul Hafidz<sup>c</sup>, Doug Haffner<sup>f</sup>, Ascelina K.M. Hasberg<sup>d</sup>, Marina Morlock<sup>b</sup>, Thomas von Rintelen<sup>g</sup>, Rachel Sheppard<sup>a</sup>, Björn Stelbrink<sup>h</sup>, Janelle Stevenson<sup>i</sup>

- <sup>a</sup> Department of Earth, Environmental, and Planetary Sciences, Brown University, 324 Brook St., Providence, RI 02912, USA
- b Institut of Geological Science & Oeschger Centre for Climate Change Research, University of Bern, Baltzerstrasse 1+3, 3012 Bern, Switzerland
- <sup>c</sup> Faculty of Mining and Petroleum Engineering, Institut Teknologi Bandung, Jalan Ganesa 10, Bandung 40132, Indonesia
- <sup>d</sup> Institute for Geology and Mineralogy, University of Cologne, Zülpicher Str. 49a/b, 50674 Cologne, Germany
- <sup>e</sup> Berkeley Geochronology Center, Berkeley, CA 94709, USA
- f Great Lakes Institute for Environmental Research, University of Windsor, Windsor, Ontario N9B 3P4, Canada
- 8 Museum f
  ür Naturkunde, Leibniz Institute for Evolution and Biodiversity Science, Invalidenstr. 43, 10115 Berlin, Germany
- <sup>h</sup> Zoological Institute, University of Basel, Vesalgasse 1, 4051, Switzerland
- <sup>i</sup> School of Culture, History and Language, Australia National University, Acton, ACT 2601, Australia

#### ARTICLE INFO

# Keywords: Southeast Asia Paleolimnology Geochemistry Sedimentology Paleoclimate Ancient lake

# ABSTRACT

There is a paucity of long and continuous continental records from South East Asia suitable to inform on past changes and underlying causes of the region's climate and associated diverse ecosystem evolution during the late Quaternary. In 2015, the Towuti Drilling Project (TDP) collected a series of sedimentary drill cores from the tectonic, ferruginous, and highly biodiverse Lake Towuti, Sulawesi, one of Indonesia's oldest lakes. The drill cores contain ~1 Myr of uninterrupted lacustrine sedimentation to document long-term environmental and climatic change in the tropical western Pacific, the impacts of geological and environmental changes on the biological evolution of aquatic taxa, and the geomicrobiology and biogeochemistry of metal-rich, ultramafichosted lake sediment. Here we use lithostratigraphic, mineralogical, geochemical, and geochronological datasets to elucidate Lake Towuti's tectonic emergence and its biogeochemical responses to climatic and volcanic forcings since lake formation. Our data document that Lake Towuti emerged during a phase of accelerated tectonic subsidence from a landscape characterized by active river channels, shallow lakes and swamps into a permanent lake at ~1 Ma. The lacustrine sediments feature quasi-rhythmic alternations of green organic rich and red sideritic clay beds reflecting changes in lake mixing and biogeochemistry as a response to temperature and hydrological changes driven by orbital-scale changes in insolation and continental ice volume through the midto late Pleistocene. Clay deposition is interrupted by two beds of diatomaceous oozes composed primarily of planktonic diatoms that reflect phases of substantially increased primary productivity. The occurrence of these diatomaceous oozes in close association with multiple tephra beds suggests a trophic state change driven by the addition of volcanically sourced P, possibly in combination with a lake mixing state that supports recycling of P. Data on lake age and ontogeny are also in agreement with molecular-clock estimates of  $\sim$ 0.7 Ma (0.18–1.37 Ma) for the divergence of Lake Towuti's Telmatherinid fishes from a riverine ancestor. Our data therefore are compatible with an evolutionary model in which Lake Towuti's endemic fauna is a result of geographic speciation in the Malili Lakes, a set of large lakes in Southeast Sulawesi, driven by physical or chemical dispersal limits imposed by the regional rivers and lakes. More detailed chronological constraints and refined climate and environmental proxy datasets are currently in preparation and will help to paint a more detailed history of the region's climate and environmental history in future studies.

E-mail address: James\_Russell@Brown.edu (J.M. Russell).

<sup>\*</sup> Corresponding author.

#### 1. Introduction

The Indo-Pacific Warm Pool (IPWP) isis home to the largest zone of deep atmospheric convection on Earth and exerts enormous influence on global climate (Cane, 2005; Chiang, 2009; Clement et al., 2001; Phillips et al., 2012). Convection over the IPWP is linked to globally important climate phenomena such as the El Niño-Southern Oscillation (ENSO), and influences the concentration of atmospheric water vapor, the Earth's most important greenhouse gas (Pierrehumbert, 2000). Our ability to understand past changes in the tropical hydrological cycle and to make accurate predictions of future changes in tropical climate therefore rests on our understanding of tropical Pacific climate under boundary conditions different from those experienced in recent time. Long drill-core records have substantially improved our understanding of the late Quaternary climate history in tropical South America and Africa (e.g. Fritz et al., 2007; Johnson et al., 2016; Lupien et al., 2018); however, proxy records of IPWP hydrology exhibit profound differences in their orbital-scale patterns that challenge our understanding of the controls on IPWP paleohydrology (Ayliffe et al., 2013; Carolin et al., 2016; Konecky et al., 2016; Krause et al., 2019; Mohtadi et al., 2011; Reeves et al., 2013; Russell et al., 2014). Thus, despite its importance, the response of Indo-Pacific hydroclimate to global climate change and forcings is uncertain.

To improve our understanding of Indo-Pacific environmental history, in 2015 an international team of scientists recovered a long and continuous sedimentary record through scientific drilling at Lake Towuti, South Sulawesi, Indonesia (the Towuti Drilling Project, or TDP; Russell et al., 2016). Lake Towuti is the largest lake within the Malili Lake System, a set of five tectonic lakes in Sulawesi (Fig. 1). Studies of shallow piston cores from Lakes Towuti and Matano have documented large hydrologic responses to global climate changes highlighted by strong drying during the last glacial maximum (LGM) reconstructed through isotopic records of terrestrial leaf waxes (Russell et al., 2014; Wicaksono et al., 2015), sediment geochemistry (Costa et al., 2015), and sedimentological reconstructions of lake level (Vogel et al., 2015).

A key goal of the TDP is to extend this record over multiple glacialinterglacial cycles to investigate IPWP hydrological change over the full range of climate boundary conditions and multiple glacial-interglacial cycles that occurred during the mid- to late Pleistocene. In addition to its paleoclimatological significance, Lake Towuti harbors endemic species flocks of snails, crabs, shrimps, and fish that evolved in situ over the lake's long history (von Rintelen et al., 2012; Vaillant et al., 2011). A major goal of the scientific drilling program is to elucidate the environmental context in which these organisms evolved. Lake Towuti and vicinity is immediately underlain by the East Sulawesi Ophiolite (Monnier et al., 1995), which releases iron and other metals that catalvze biogeochemical reactions by an exotic microbial community in the lake and its sediments (Crowe et al., 2008b; Haffner et al., 2001; Vuillemin et al., 2016). Understanding the biogeochemistry of these sediments can provide insight into processes that prevailed in ancient ferruginous oceans on early Earth (Crowe et al., 2008a; Crowe et al., 2014). However, the Eurasian, Indo-Australian, Caroline and Philippine Sea plates converge at Sulawesi, giving rise to a variety of crustal processes (Hall and Wilson, 2000; Hamilton, 1979; Spakman and Hall, 2010) that influence Towuti's sedimentary record. Developing paleoenvironmental reconstructions from Lake Towuti requires disentangling the impacts of tectonics and climate, as well as geomicrobiological and diagenetic impacts, on the lake's sediments.

Here we present the first detailed sedimentological, geochemical, and biogeochemical analyses of the  $\sim 1.1~\rm km$  of sediment core recovered by the TDP. We use these records and new analyses of shallow piston cores to unravel the tectonic, climatic, and biogeochemical processes controlling sedimentological change in these cores, and in particular how climate and tectonics have influenced the biogeochemistry and mineralogy of this sedimentary succession. We document profound changes in this lake ecosystem during the past  $\sim 1~\rm million~years~(Ma)$ , which have impacted the lakes' endemic organisms. This study establishes a framework for future investigations of the midto late Pleistocene paleoclimatic history of this region.

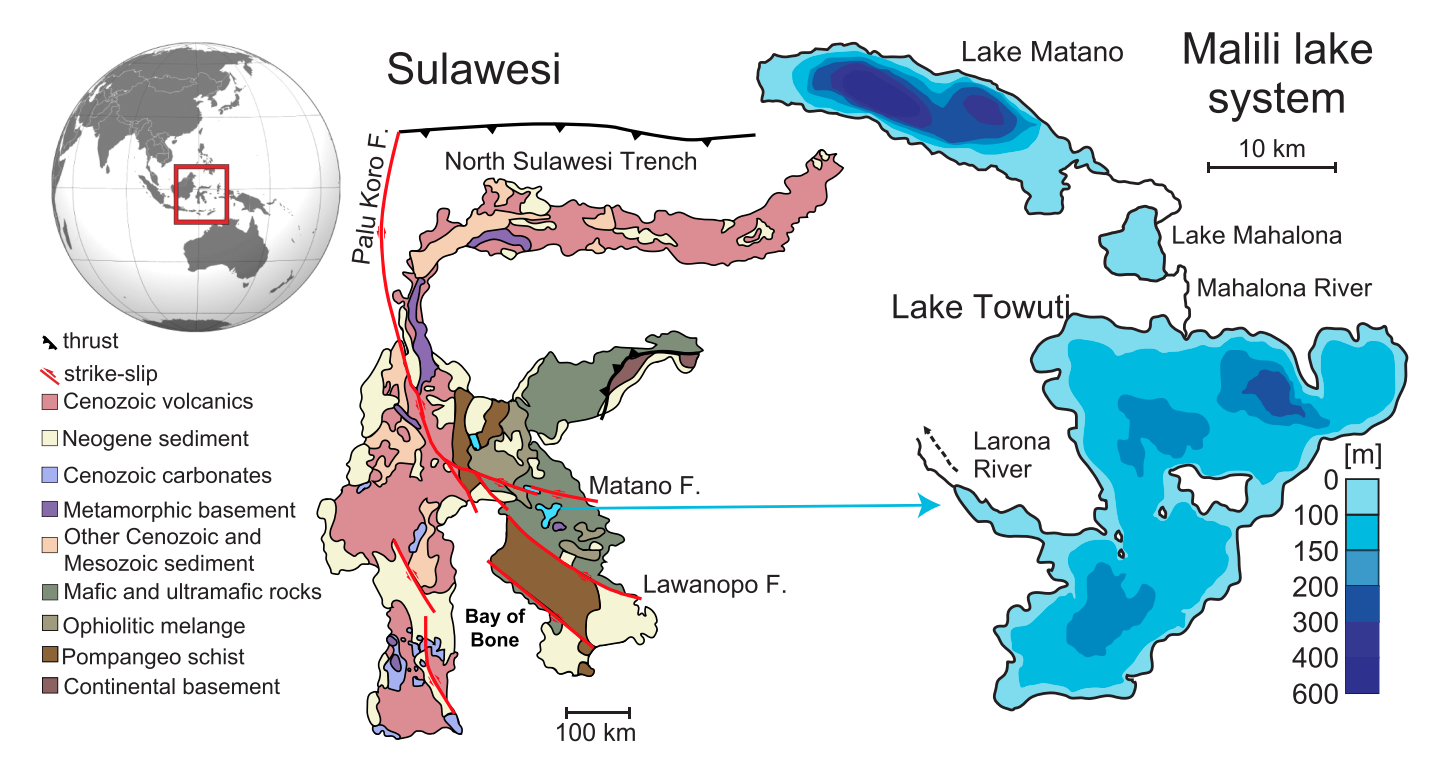


Fig. 1. Maps showing the location of Sulawesi within Indonesia (upper left), major faults and the bedrock geology of Sulawesi (center, modified from Hall and Wilson, 2000), and the bathymetry of the Malili Lakes (right), modified from Russell et al. (2016). In the geological map, transform faults are red, and subduction zones are black. (For interpretation of the references to color in this figure legend, the reader is referred to the web version of this article.)

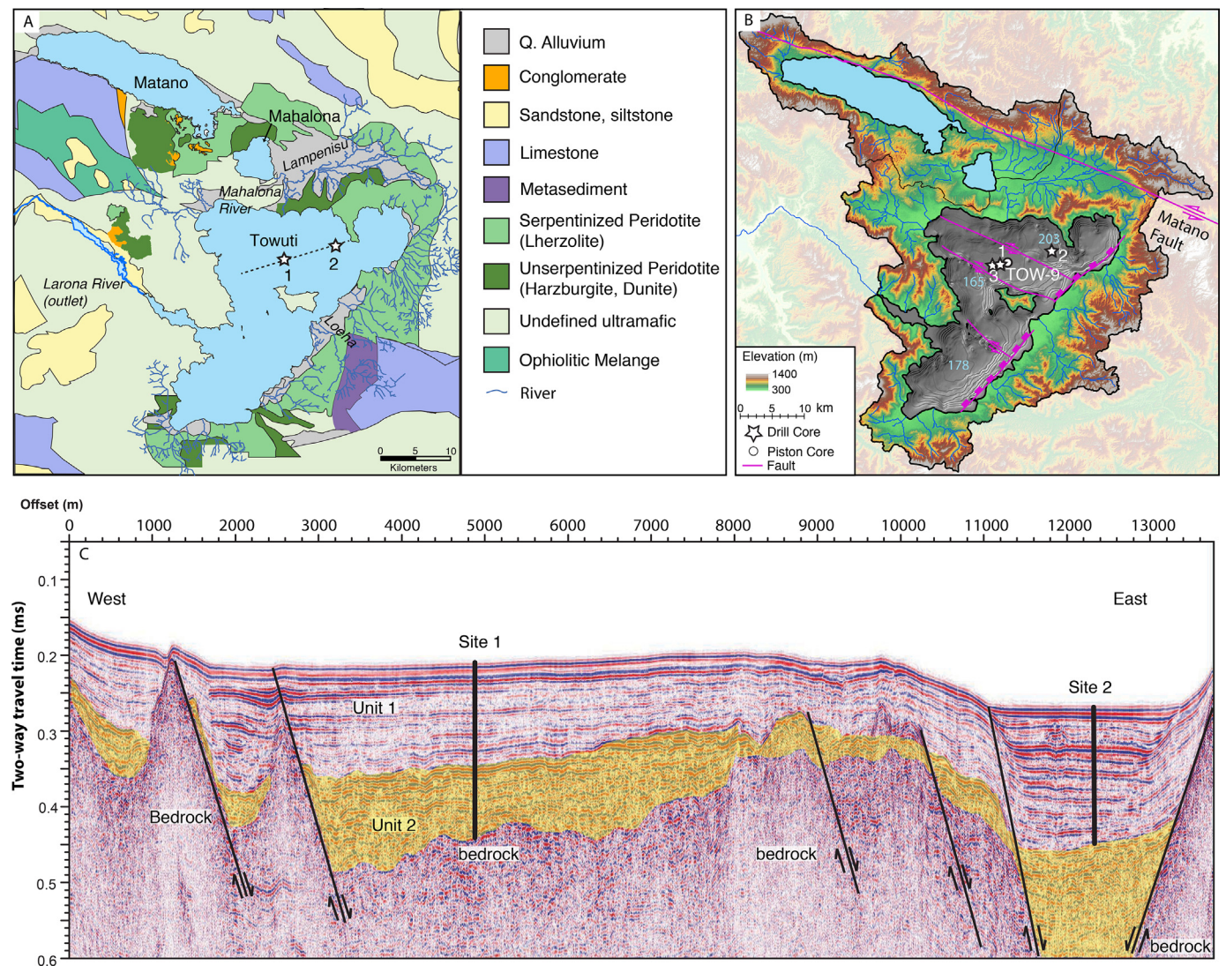


Fig. 2. At upper left, a map of the local geology of Lake Towuti's catchment modified from Costa et al. (2015). Drill sites are marked with stars, and the dashed line in the lake indicates the location of the seismic line shown in the lower image. Upper right: elevation map and bathymetric map of Lake Towuti. Grey color is sun shading to illustrate basin topography; grey lines are 25-m depth contours. The maximum depth within each of the lake's sub-basins is indicated in light blue text. Drill sites, the coring location of TOW-9, and major faults in the lake are marked. Lower panel: airgun seismic reflection line over drilling sites 1 and 2 with faults labeled. (For interpretation of the references to color in this figure legend, the reader is referred to the web version of this article.)

#### 2. Regional setting

#### 2.1. Geological background

The island of Sulawesi, in eastern Indonesia, is composed of four elongate 'arms', which broadly correspond to lithotectonic units (Fig. 1; e.g. Hall and Wilson, 2000; Hamilton, 1988; Watkinson, 2011). Lake Towuti is located on the southeast arm of Sulawesi, and its catchment is underlain by the Eocene East Sulawesi Ophiolite, comprised of mafic and ultramafic rocks (Hamilton, 1979; Monnier et al., 1995; Fig. 2A). The ophiolites have sourced lateritic nickel deposits that attracted the mining industry beginning in the 1970s, currently operated by PT Vale Indonesia (PTVI). The northeast arm of Sulawesi is formed from convergence between the Philippine Sea Plate and Sundaland, leading to extensive volcanism (Hall, 2017; Spakman and Hall, 2010).

Three major strike-slip fault systems dissect Sulawesi: the Palu-Koro (PKF), Matano, and Lawanopo Faults (Fig. 1; Hamilton, 1979). Sinistral slip along the PKF accommodates clockwise rotation and northward movement of eastern Sulawesi relative to Sundaland, with slip rates estimated at 34 mm/yr (Walpersdorf et al., 1998). The Matano Fault

(MF) is linked to the PKF (Hamilton, 1979), and rotational movement generates both lateral and vertical (extension) motion along the MF that accommodates Lakes Towuti and Matano (Fig. 2B). The Malili Lakes are postulated to have formed from these processes in the last 1.5–2 million years (Myr) (Brooks, 1950). Ahmad (1977) correlated limestone units on either side of a 90-km-long strand of the MF south of Lake Matano, and estimated an age for the lake of  $\sim$ 2 Ma based upon this lateral displacement assuming a fault slip rate of 1 cm/yr. However, lateral stream offsets have since been observed along the fault trace suggesting a high level of young activity (Bellier et al., 2006) that could imply a younger age of the lakes.

# 2.2. Climate and hydrology

Lake Towuti is located near the equator (2.75°S, 121.5°E) with a surface 318 m above sea level. The region experiences a tropical humid climate (Fig. 3). Regional precipitation averages 2700 mm/yr at the elevation of Lake Towuti, with higher rates at higher elevations. Precipitation is strongly controlled by coupled interactions between the Australian-Indonesian winter and summer monsoons, regional sea

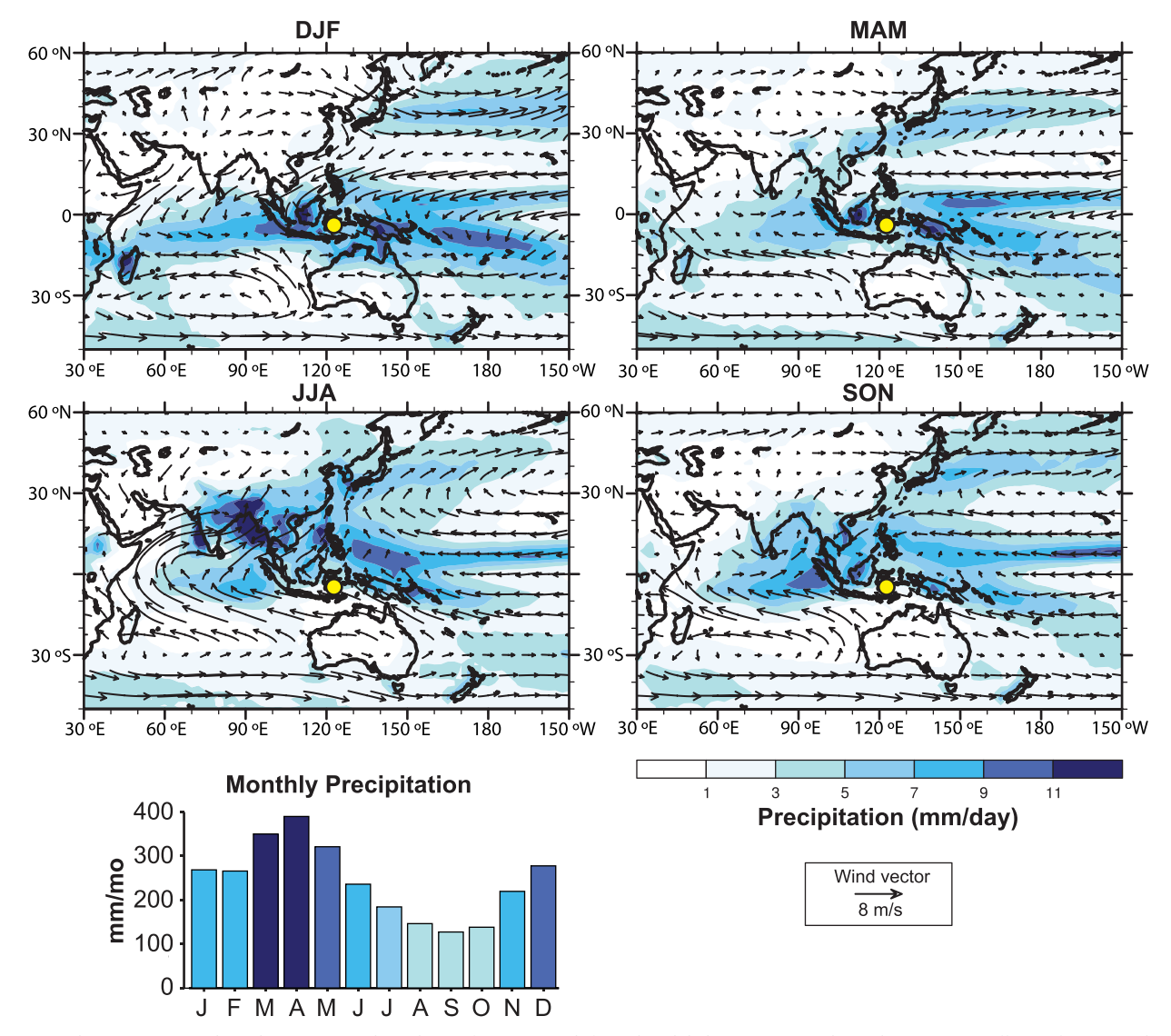


Fig. 3. Seasonal precipitation and wind vectors over the Indo-Pacific Warm Pool, from the Global Precipitation Climatology Project (Adler et al., 2016). The yellow circle marks the location of Lake Towuti. Lower left panel shows monthly precipitation values from observations at the shore of Lake Towuti from 2013 to 2018, modified from (Konecky et al., 2016). The color code is the same as for the GPCP data. (For interpretation of the references to color in this figure legend, the reader is referred to the web version of this article.)

surface temperatures, and the strength and position of the Intertropical Convergence Zone (ITCZ; Aldrian and Susanto, 2003; Hendon, 2003). South Sulawesi experiences a wet season from December to May as the ITCZ migrates southward over Indonesia, and the Australian-Indonesian Summer Monsoon (AISM) drives strong northeasterly flow into Sulawesi. During this time warm local sea surface temperature and strong local convective activity result in regional precipitation in excess of 250 mm/month (Konecky et al., 2016). Precipitation falls below 150 mm/month from July-October, when the ITCZ migrates northward toward mainland Asia, and cool sea surface temperatures suppress convection. This seasonal precipitation pattern is generally similar to much of southern Indonesia (Aldrian and Susanto, 2003). Interannual variability in precipitation over Sulawesi is governed by variations in the monsoons, sea surface temperatures (SSTs), as well as interannual variability in ENSO (Aldrian and Susanto, 2003). Indeed, strong drying during the 1997-1998 El Niño event resulted in a lake level decline of ~3 m, to near the outlet sill depth of Lake Towuti, and thus caused a shift to closed-basin conditions (Tauhid and Arifian, 2000).

Lake Towuti is the largest of the Malili Lakes, with a surface area of 560 km<sup>2</sup> and a maximum water depth of 203 m (Haffner et al., 2001; Lehmusluoto et al., 1995). The three largest of the Malili Lakes, Matano,

Mahalona, and Towuti, are connected with surface outflow from Matano to Mahalona to Towuti, which drains into the Bay of Bone via the Larona River. The Mahalona River drains Lakes Matano and Mahalona, as well as the catchment of the Lampenisu River, which converges with the Mahalona River between Lake Mahalona and Lake Towuti, and is by far the largest river input to Lake Towuti (Fig. 2B).

Lake Towuti occupies a mountainous catchment area of ~1144 km² that can supply sediment to the lake (Fig. 2B), plus the 500 km² combined catchments of Lake Matano (surface area of 160.5 km²) and Lake Mahalona (22.2 km²) that can supply water. PT Vale Indonesia (PTVI) operates a large hydroelectric dam on Lake Towuti's outlet, which provides measurements of the lake's outflow (4.19 km³/year; Tauhid and Arifian, 2000). Using the Penman method (Penman, 1948) and shoreline meteorological data we estimate annual evaporation from Lake Towuti's surface of 1.3 m (a volume of 0.73 km³/year). As Lake Towuti's water level is relatively stable, these water losses must be balanced by inflows from the catchment and direct precipitation onto the lake surface. River- gauge measurements are not available from all of Lake Towuti's inflows, but precipitation onto the lake surface is ~1.51 km³/year based on shoreline precipitation measurements (2700 mm/yr; Konecky et al., 2016), implying inputs from the

catchment must total  $\sim 3.42~{\rm km}^3/{\rm yr}$ . Assuming precipitation over the entire catchment area of Lakes Towuti, Matano, and Mahalona is 2700 mm/year (which is likely an underestimate given increasing precipitation at higher elevations), we estimate the Mahalona River flow is  $\sim 1.79~{\rm km}^3/{\rm yr}$ , with the remaining  $1.63~{\rm km}^3/{\rm yr}$  derived from rivers entering Towuti's eastern, southern, and western shorelines. These estimates imply a water yield coefficient (inputs from the catchment relative to precipitation of 0.7, slightly higher than but generally similar to yield coefficients estimated for tropical forests in Kalimantan (0.5–0.6, Suryamoto et al., 2013).

#### 2.3. Modern sedimentation and limnology

Bedrock in the Lake Towuti catchment is primarily comprised of mafic to ultramafic rocks, with limited exposure of marine sediments and metasediments (Fig. 2A; Costa et al., 2015; Kadarusman et al., 2004). Serpentinized peridotite (lherzolite) dominates toward the east and northeast of Lake Towuti, whereas unserpentinized ultramafic rocks occur to the north of Lake Towuti. Siliciclastic sedimentary and metasedimentary bedrock occurs to the east. Quaternary alluvium, which is largely composed of weathered mafic rock, covers major river valleys to the north and northwest of Lake Towuti (Fig. 2A). Chemical and mineralogical analyses of laterite soil profiles document a typical weathering succession with high Mg and serpentine concentrations at the transition between ultramafic bedrock and weathered substrates at the base of the soil (Morlock et al., 2018). Conversely, top soils are residually enriched in Fe, Al, and Ti primarily bound in or adsorbed onto Fe-oxyhydroxides and secondary phyllosilicates (smectite, kaolinite) and more resistant mineral phases (rutile, zircon, spinel; Morlock et al., 2018; Sheppard et al., 2019).

These catchment bedrock compositions leave a strong imprint on sediments in Lake Towuti (Costa et al., 2015; Goudge et al., 2017; Hasberg et al., 2018; Morlock et al., 2018; Sheppard et al., 2019). The Mahalona River and its largest tributary, the Lampenisu River, drain catchments primarily composed of serpentinized peridotite and ultramafic-derived Quaternary alluvium and supply the majority of sediment rich in Mg and serpentine to Towuti's northern basin (Costa et al., 2015; Goudge et al., 2017; Hasberg et al., 2018). The Loeha River (Fig. 2a) and smaller rivers draining the limestone and metasedimentary bedrock to the east deliver sediments with a more felsic signature enriched in K, kaolinite, and quartz. Smaller rivers drain catchments dominated by ultramafic bedrock in the northeast and southwest and supply sediments enriched in Fe, Cr, and Ni, likely derived from topsoil erosion.

The waters of Lake Towuti are relatively dilute (210  $\mu$ S/cm) and circumneutral (Haffner et al., 2001; Lehmusluoto et al., 1995) and is among the least productive tropical lakes on Earth (Sabo et al., 2008), likely a result of sedimentary PO<sub>4</sub><sup>3-</sup> trapping by the very high sedimentary Fe oxyhydroxide concentrations (Vuillemin et al., 2016, 2020).

Monitoring of the lake's thermal structure from August 2012 until May 2015 showed that the lake never mixed completely during that time, with surface temperatures from ~28.5 to ~30.5 °C and temperatures below ~100 m depth consistently near 28.0 °C (Costa et al., 2015). The lake surface is warmest during the wet season (30.5 °C, March–May) and coolest during the dry season (28.5 °C, August–October), during which time the upper 100 m of the water column undergoes isothermal mixing. During the dry season the loss of latent heat from the lake to evaporation cools the lake surface, and the upper 100 m of the water column becomes nearly isothermal and mixes. The waters below 100 m depth are hypoxic to anoxic, with elevated concentrations of reduced metals (e.g.  ${\rm Fe}^{2+}$ ; Costa et al., 2015; Vuillemin et al., 2016).

Sarasin and Sarasin (1895) were the first to document the lakes' unique, endemic fauna. We now have basic biological data (taxonomic and molecular genetic data) for many groups including fishes (sailfin silversides, gobies, ricefish), snails, shrimps, crabs, and sponges that

indicate the extent of biological endemism and complexity of biological innovation and speciation (i.e. adaptive radiation) in these systems (von Rintelen et al., 2012). The Malili Lakes harbor at least 51 species of fishes, dominated by 31 species of silversides, as well as 45 species of snails, 14 species of shrimps, and several other species-rich but less well-investigated taxa. Molecular-clock estimates suggest that most of these species flocks originated ~2 Ma or later, though the uncertainties on these estimates are very large (on the order of 1 Ma) due to uncertainties in appropriate sister groups and mutation rates (e.g. Stelbrink et al., 2014). There is a high degree of habitat and substrate specialization in the lakes' fauna, from structures of the snails' radulae for feeding on hard vs. soft substrates (von Rintelen et al., 2012), to claw-bearing leg and pharvngeal jaw modifications in shrimps and sailfin silversides, respectively (Herder et al., 2006; von Rintelen et al., 2012; Roy et al., 2004). Interestingly, despite the fact that Lakes Matano, Mahalona, and Towuti are linked by rivers, there is a high degree of biological endemism within each lake, not just in the Malili system (von Rintelen et al., 2012). Approximately 60% of the fishes and snails that live in Lake Towuti are endemic to this lake only. Similarly, the diatom communities of the lakes also contain many endemic pennate diatoms, and the diatom communities are very different from lake to lake with only 5 species of over 200 identified taxa common to all lakes (Bramburger et al., 2006; Bramburger et al., 2008).

#### 3. Basin framework and drill-core site selection

#### 3.1. Acoustic and piston coring surveys

Between 2007 and 2013 we collected ~250 km of high-resolution seismic reflection (CHIRP) data using an Edgetech™ 3200 high-penetration sub-bottom profiling system with an SB-424 towfish, and deeper seismic reflection data including both single channel and multichannel data using a Bolt™5 in³ airgun and a 150-m-long Geometrics™GeoEel solid digital streamer with 24 channels (Russell et al., 2016; Hafidz et al., in revision). These data allowed us to situate sediment cores and drill sites within a broader stratigraphic framework to evaluate the structure and distribution of the basin and its sediments, and to detect erosional truncations indicating lake level variations. In 2010 we collected eleven 7- to 19.8-m-long cores from locations spread across the lake using modified Kullenberg and UWITEC piston corers (Russell et al., 2014; Vogel et al., 2015).

The seismic data revealed two major sedimentary units in Lake Towuti (Fig. 2C). Unit 1 consists of well-stratified sediment that extends from the lake floor to a depth of  $\sim \! 100$  m. It is characterized by parallel acoustic reflectors that can be traced across most of the basin. These reflectors do not exhibit obvious contacts, such as erosional truncation, that would indicate lake desiccation within Unit 1, but onlapping structures in the upper 10 m suggest lake level changes of up to 30 m (Vogel et al., 2015).

Unit 2 varies between a few tens to  $\sim 150$  m in thickness and is characterized by relatively discontinuous, sub-parallel reflectors. Unit 2 can be differentiated from basement by the presence of sub-parallel reflectors versus the more chaotic, often structureless bedrock. The seismic data also reveal that the Mahalona River generates a large sublacustrine delta that extends nearly 10 km from the river mouth eastward into Lake Towuti's deepest basin and southward to the intrabasinal fault that bisects the northern part of the lake (Vogel et al., 2015, Hafidz et al., in revision). The sediment in this delta must largely derive from the 300 km² Lampenisu River catchment, which merges with the Mahalona River between Lake Towuti and Lake Mahalona.

The seismic data document fault structures within Lake Towuti that play an important role in sediment distribution. The lake is dissected into three major sub-basins by large intrabasinal strike-slip faults exhibiting up to tens of meters of relief in the modern lake floor (Fig. 2b). These faults play an important role in controlling sediment distribution within the lake (Hasberg et al., 2018; Morlock et al., 2018). For

example, the northern half of Lake Towuti is bisected by a long strike-slip fault (Fig. 2b). Relief along this fault (e.g. 9000–11,000 m, Fig. 2C) bounds a deep graben structure in the north of the lake. This fault isolates sediment sourced from the northern part of the lake catchment, including the Mahalona River delta, in the northern basin of the lake (Vogel et al., 2015; Hafidz et al., in revision).

#### 3.2. Drill-core site selection and drilling operations

Analyses of sediment piston cores show that sedimentation in Lake Towuti is highly sensitive to shifts in climate. Proxy records of vegetation and sediment erosion and transport derived from a piston core (IDLE-TOW10-9B, hereafter TOW-9) from the center of Towuti's northern basin documented wet conditions during Marine Isotope Stage (MIS) 3, from ~60 to ~37 thousand years (ka), drier conditions during MIS 2, and a return to wetter conditions beginning at 16.5 ka during the last global deglaciation (Russell et al., 2014). Trace element data measured in this core indicated enhanced lake mixing during MIS 2, likely due to a stronger dry season and enhanced evaporative cooling (Costa et al., 2015). Piston cores from Towuti's deepest basin (TOW-4 and Co-1230, located near Site 2, Fig. 2) documented a large increase in the frequency of mass wasting deposits (turbidites) during MIS2 recording remobilization of Mahalona River delta topset beds and forced delta progradation in response to a  $\sim$  10-30 m drop in lake level (Goudge et al., 2017; Vogel et al., 2015).

Based on these findings, we identified three primary target sites for continental drilling (Fig. 2B, C). Site 1 was drilled from 156 m water depth near the TOW-9 core-site to provide a "master record" of Lake Towuti's history. Five holes were drilled at this site (TDP-TOW15-1A, 1B, 1D, 1E, and 1F). Site 2 was selected in Towuti's northern basin in ~200 m water depth, near the TOW-4 and Co-1230 core-sites, to recover a record of lake level and Mahalona River inflow dynamics (c.f. Vogel et al., 2015), to the Unit1/Unit 2 boundary. Three holes were drilled at this site (TDP-TOW15-2A, 2B, 2C). Site 3 was drilled a few km east of Site 1 in 159 m water depth in 2 holes (TDP-TOW15-3A, 3B). More information about the drilling operations can be found in Russell et al. (2016).

#### 4. Methods of sediment core analysis

#### 4.1. Initial core description and processing

All cores were scanned for their geophysical properties (magnetic susceptibility, density, p-wave velocity, electrical resistivity, and natural gamma radiation) using a Geotek™whole-core multisensor core logger (MSCL) upon arrival at the U.S. National Lacustrine Core Facility (LacCore). All cores were split, visually described (color, bedding, grain size, lithology), imaged using a Geotek™MSCL, and scanned for magnetic susceptibility (MS) at 0.5 cm resolution on a Geotek™ XYZ core logger. Smear slides were made from all cores at 20-50 cm resolution by dispersing sediment on a microscope slide in water, drying the specimen, and mounting the slide in optical resin. Smear slides were analyzed using a petrographic microscope to determine major sedimentary components (major minerals and grain size, microfossils, and other sediment constituents). We used the MS, visual logs, and smear slide datasets to define the most common sedimentary lithotypes, visually correlate cores between adjacent holes at each drill site to obtain a composite sediment stratigraphy, and to correlate sediment drill cores to the ~10-m Kullenberg piston cores. Results from the cores are reported in meters composite depth (mcd), except where otherwise noted.

#### 4.2. Sedimentological, geochemical, and mineralogical analyses

The composite stratigraphy from Site 1 was sampled at  $\sim$ 48 cm resolution in Unit 1 and at variable intervals (average of 56 cm resolution) in Unit 2 to evaluate compositional changes between major

sedimentary lithotypes. TOW-9 was sampled at 8 cm resolution. Except where otherwise noted, the data are derived from TOW-9 and the composite Site 1 stratigraphy (consisting of TDP-TOW15 Sites 1A, 1B, 1D, 1E, and 1F).

All sediment sub-samples were freeze-dried and homogenized using a mortar and pestle. Total carbon and nitrogen content were determined at Brown University using a CE Instruments NC2100 elemental analyzer, and inorganic carbon content (TIC) was determined using a UIC Inc. CM5014 coulometer equipped with a CM5240 automated sample acidification system. The difference between total and inorganic carbon was calculated to determine organic carbon (TOC) content. Nitrogen concentrations were extremely low (less than 0.05%) in many samples, creating considerable relative error and limiting our ability to estimate OM quality and source using organic carbon to nitrogen (C/N) ratios. Because of this, and to support future organic geochemical studies of the cores, we extracted free lipids from the sediments using a Dionex™ Accelerated Solvent Extractor (ASE) 350 using a 9:1 dichloromethane:methanol solution. The total lipid extracts (TLE) were gently dried using nitrogen gas, and weighed. We use the weight of the TLE relative to the organic carbon content of the sample to estimate OM quality, with higher TLE:TOC ratios indicating more abundant free lipids and hence less degraded OM. We analyzed the carbon isotopic composition of OM  $(\delta^{13} \bar{C}_{OM})$  on a Costech Instruments elemental combustion system coupled to a Delta V Plus isotope ratio mass spectrometer via a Conflo II interface. Aliquots of each sample were pretreated by soaking in 1 N H<sub>2</sub>SO<sub>4</sub> for 2 h at room temperature to remove inorganic carbon prior to analysis of  $\delta^{13}C_{OM}$ . Precision on standards and 10% sample replication were 0.116%. We tested this method on carbonate-free sediments from TDP (n = 10) to examine whether acidification affected the  $\delta^{13}C_{OM}$  and observed no changes exceeding our analytical precision (Supplemental Information).

Major element concentrations were analyzed through the upper 100 m of sediment at Site 1 by digesting samples using flux fusion followed by analysis using inductively coupled plasma atomic emission spectroscopy (FF-ICP-AES) based upon the procedure outlined in Murray et al. (2000). In addition, we measured the reactive iron concentrations in a subset of samples from TOW-9 using a two-step modified version of the sequential extraction protocol from Poulton and Canfield (2005), as described by Sheppard et al. (2019). Powdered sediment samples were leached in hydroxylamine hydrochloride for 48 h at room temperature. After removing the supernatant and rinsing the sample with deionized water, the sediment was leached in sodium dithionite for 2 h at room temperature. The supernatants were combined and their Fe concentrations measured to determine the concentration of reactive Fe. All samples were analyzed on a Jobin Yvon 2000 ICP-AES. Concentration data are calibrated to fluxed standard reference materials following blank and drift corrections. Major element concentrations were also analyzed in dried and powdered samples using an XRF core scanner (ITRAX, Cox Ltd., Sweden) equipped with a chromium anode X-ray tube (Cr-tube) set to 30 kV, 50 mA at the University of Bern. Samples were placed in 2 imes 2 cm sample containers and measured using 2 mm integrals and 50 s integration time (e.g. Morlock et al., 2018). These analyses provide elemental concentrations for the lowermost ~60 m of sediment at Site 1.

Relative concentration changes of serpentine and quartz were assessed using Fourier Transform Infrared Spectroscopy at the University of Bern. Sample preparation, instrument configuration, and data processing were performed according to Vogel et al. (2016). Measurements were performed using a Bruker Vertex 70 equipped with a liquid-N<sub>2</sub>-cooled MCT (mercury–cadmium–telluride) detector, a KBr beam splitter and a HTS-XT accessory unit (multisampler). Peak areas diagnostic for symmetric stretching of SiO<sub>4</sub> in quartz (778 cm $^{-1}$ ) and bending vibrations of OH in serpentine group minerals (640 cm $^{-1}$ ) and representative for their relative abundance in Towuti sediments (e.g. Morlock et al., 2018) were integrated using the OPUS (Bruker) software package.

#### 4.3. Age determination in the Lake Towuti cores

The chronology for TOW-9 has been previously published (Russell et al., 2014). It is constrained by 20 AMS <sup>14</sup>C ages on bulk organic carbon and 3 ages measured on terrestrial macrofossils to constrain the combined effects of organic matter reworking, <sup>14</sup>C reservoir effects, and other sources of "old carbon" to the sediment. <sup>14</sup>C ages were calibrated using Calib 6.0 (Reimer et al., 2009), and depth-age relationships were modeled using a mixed-effect regression that incorporates both age and model error (Russell et al., 2014). For sediments beyond the <sup>14</sup>C timescale, we extrapolated the average sedimentation rate over the <sup>14</sup>C-dated interval. In this paper we do not interpret the timing of events beyond the <sup>14</sup>C-dated interval. Because the stratigraphy of Lake Towuti drill cores at Site 1 are near identical to TOW-9, we transferred these <sup>14</sup>C ages from TOW-9 to the Site 1 composite stratigraphy through correlation of their MS profiles (Supplemental Fig. S1) and by aligning marker beds such as red and green clays (see below).

In addition to these radiocarbon ages, the 40Ar/39Ar dating method was used to date a 2-cm-thick sanidine-bearing ash (tephra 18, T18) at 72.95 mcd. Two samples of T18 were taken from two Site 1 cores and were washed gently through new 60 µm sieves, dried, and hand-picked to obtain sanidine crystals in the ~100-250 µm size range. After separation, the mineral concentrates were irradiated for one hour in the Oregon State University TRIGA reactor. Sanidine phenocrysts from the Alder Creek Rhyolite of California with an age of 1.1848  $\pm$  0.0006 Ma (Niespolo et al., 2017) were used as the neutron fluence monitor. Following radiological cooling after irradiation, the sanidine was analyzed using two variants of the 40Ar/39Ar dating technique using a CO<sub>2</sub> laser as the heating instrument: single-grain total fusion (SCTF), in which a grain is fused in a single step with a focused beam to release all trapped gasses, and single-grain incremental heating (SCIH), in which an individual grain is heated with a diffuse beam in progressively increasing steps until all gasses are released. Argon gas measurements were performed at the Berkeley Geochronology Center on a 5-collector Nu Instruments Noblesse noble-gas mass spectrometer operating in simultaneous ion-counting mode. Additional details of the general analytical and data-reduction process are provided in Deino et al. (2018) and the supplemental text.

# 5. Results

# 5.1. Sedimentary lithotypes, stratigraphy, and chronology

Lithostratigraphy at Site 1 can be readily correlated between the holes (A-F) based on visual appearance and relative position of sediment beds, and define a composite stratigraphy that is > 99% complete through the upper 140 m but more discontinuous between 140 m and bedrock (Fig. 4). The complete succession can be separated into two major units. Lower Unit 2 overlies bedrock at 162.8 m and transitions into Unit 1 at 98.9 mcd (Fig. 2C, 4). The base of the TDP Site 1 hole consists of a completely lithified mafic conglomerate, which is overlain by an consolidated ~20-cm-thick reddish-brown, dry, clayey silt. The sediments overlying these deposits in Unit 2 are composed of four lithotypes distinguished by their grain size, mineralogical composition, and TOC content (Fig. 4). In Unit 2, grain size ranges from silt to gravel with less than 50% contribution from clay. The lowermost ~10 m consist of massive to thickly bedded mafic sand and gravel that grade quickly into sandy beds (Fig. 4). Above this, medium to thickly bedded silts with occasional sandy beds dominate. The silts differ in color, ranging from green-grey to blue-grey, with the greenish silts primarily composed of mafic minerals and the blueish silts of felsic mineral assemblages (Fig. 5). Siderite is common in Unit 2, often forming 1-cm and larger concretions. Medium bedded to massive woody peats are interspersed with the clastic lithologies and form the topmost bed of Unit 2 (Fig. 4). At Site 1, this woody peat is capped by an  $\sim$ 1-m thick silt. Although unconformities are observed at the Unit 1/Unit 2 boundary in seismic reflection data elsewhere in the basin (e.g. 6500–8000 m, Fig. 2C), this transition appears conformable at Site 1.

Unit 1 comprises the upper 98.9 m of the succession at Site 1 and is predominantly fine-grained with clay comprising 60-90% by volume. Three major lithotypes can be distinguished in Unit 1 based on differences in color, structure, siderite, and TOC content: green clays, red sideritic clays, and diatomaceous ooze (Figs. 4, 5). Green clays and red sideritic clays dominate the Unit 1 succession. Green clays are dark, thin to medium bedded, and have higher TOC concentrations than the sideritic clays. Sideritic clays are thin to medium bedded to mottled, and siderite occurs both finely dispersed in the sediment matrix and in discrete layers, lenses, and concretions, the latter of which become more abundant between 70 and 90 mcd. There are two 3-5 m thick beds of dark olive grey, laminated to massive diatomaceous oozes between ~45 and ~ 32 mcd. In addition, we observe two lithologies originating from event deposits: 2-50 cm thick normal-graded turbidite beds, and 25 thin to medium (~1-20 cm) tephra beds. Turbidites are relatively infrequent at Site 1. With one exception at 114 mcd, tephras occur between ~95 and ~ 18 mcd, and are particularly frequent between 70 and 40 mcd.

Variations in the abundance of major elements including Mg and K track changes in the detrital mineral (quartz, serpentine) composition of the Site 1 succession and indicate changes in sediment sources related to the tectonic and geomorphic evolution of the lake (Fig. 5). Quartz and serpentine abundance are generally antiphased, with quartz positively correlated to K and serpentine to Mg, as has been observed in surface sediment samples (Morlock et al., 2018). Quartz content is generally highest in Unit 2. Both quartz and serpentine, and Mg and K, are elevated at the base of Unit 1, and decline between ~85 and 75 mcd when Fe concentrations rise. Quartz and K concentrations are relatively stable from 75 to ~30 mcd, where %Mg is low and serpentine content is below detection limits. Serpentine and Mg rise substantially at ~30 mcd. Based on these data, we divide Unit 1 into three lithologic subunits, 1c-1a (Figs. 4, 5), discussed below.

The lithostratigraphy and MS profile observed at Site 1 is very similar to Site 3, though the latter is slightly expanded and contains more frequent and thicker turbidites (Fig. 6 and Supplemental Fig. S2). This could be due to the position of Site 3 slightly closer to the steeply sloping southeastern shoreline, assuming the turbidites are derived from the south. The succession at Site 2 extends to 136.4 mcd, and terminates in a coarse sand. We estimated the Unit 1 thickness at Site 2 to extend to  $\sim\!130$  mcd from the seismic reflection data, so it appears our core captured the Unit 1 sediments. The lower  $\sim\!76$  m of Site 2 is very similar to Site 1, but the upper 60 m of Site 2 contains green and red clays interbedded with very frequent turbidites sourced from the Mahalona River Delta. The turbidites are normal graded beds between 1 and  $\sim$  50 cm thick, with coarse to fine sand bases that grade into silts and clays.

We have correlated sediments of Unit 1 at Sites 1–3 on the basis of visually distinct tephras, distinct sedimentary features such as the diatom oozes, and MS profiles (Fig. 6). Site 3 is very similar to Site 1, but Unit 1 at Site 3 is expanded by  $\sim\!5\%$  owing to the more frequent occurrence of thicker turbidites. The lower 76 m of Site 2 is similar to Site 1, but the upper 60 m of Site 2 is expanded by  $\sim\!250\%$  relative to Site 1, due to the frequent turbidites. The onset of turbidite deposition at Site 2 occurs just above Tephra 2 (Fig. 6), which is near the onset of high %Mg and high serpentine content at  $\sim\!30$  mcd at Site 1 (Fig. 5). The lower  $\sim\!18$  m of sediment in Unit 1 at Site 1 also appear to be absent from Site 2 based on visual comparison of the lithologies and the MS profiles at both sites.

AMS <sup>14</sup>C ages indicate an age of ~44.7 ka at 9.79 m, implying a sedimentation rate of 0.219 m/kyr in the upper Unit 1 at Site 1. Extrapolation of this sedimentation rate to the base of Unit 1 would suggest a basal age of ~450 ka. However, the  $^{40}$ Ar/ $^{39}$ Ar dating results on T18 at 72.95 m yielded an age of 797.3  $\pm$  1.6 ka (see Supplemental Text and Figs. S3-S8 for  $^{40}$ Ar- $^{39}$ Ar results), indicating a much slower

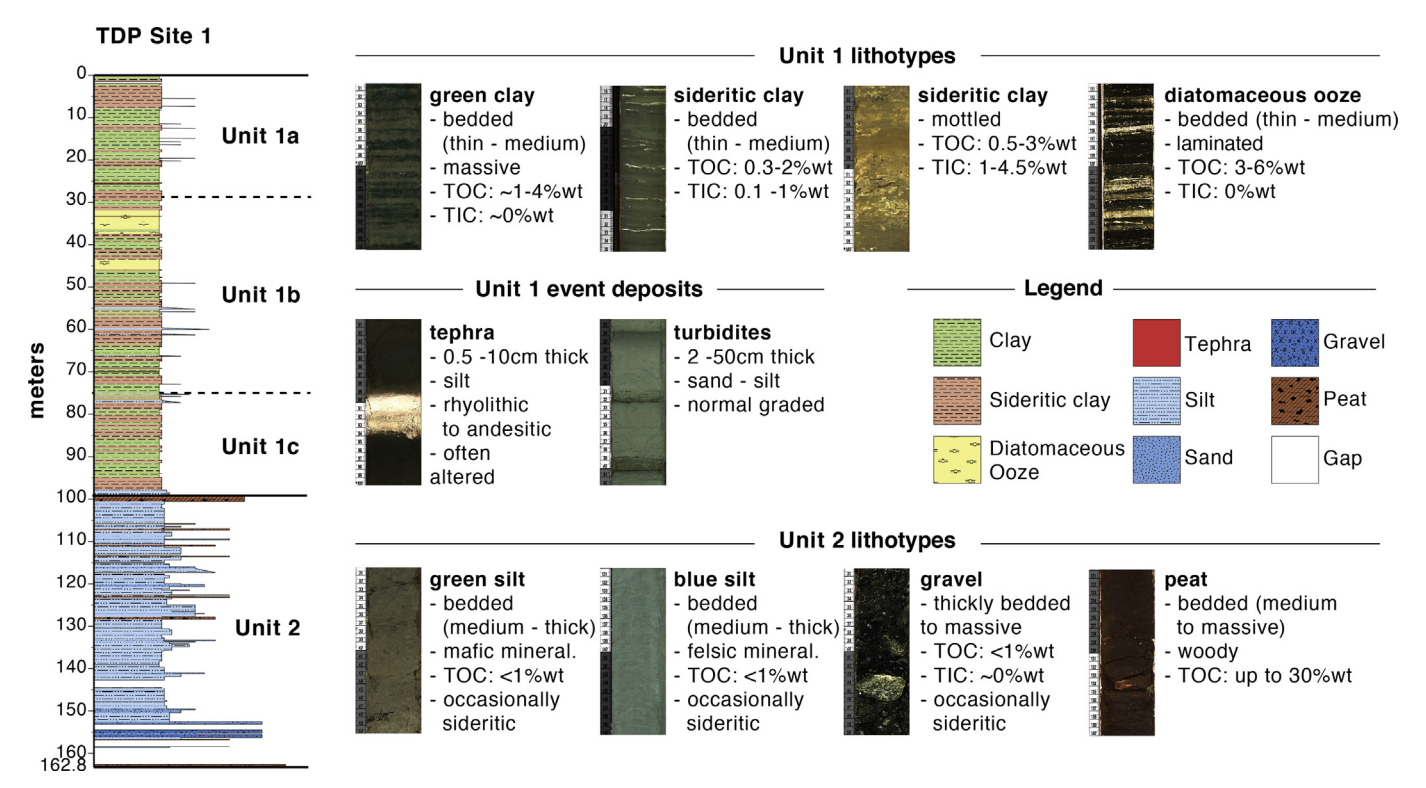


Fig. 4. The composite lithostratigraphy from TDP Site 1, together with the major lithotypes present in this sequence.

sedimentation rate in the lower parts of Unit 1 at Site 1.

# 5.2. The geochemical stratigraphy of TOW-9 and Site 1

Piston core TOW-9 from Lake Towuti, spanning the last  $\sim\!60$  ka, is comprised of alternating thinly bedded green clays and more massive to

mottled red sideritic clays (Fig. 7) (Russell et al., 2014). In core TOW-9, the red sideritic clays are marked by  $\sim\!\!20\%\text{Fe}$ , which includes  $\sim\!\!8\%$  reactive Fe, high %Siderite and  $\delta^{13}C_{OM}$ , and low %TOC and TLE/TOC. In TOW-9, this red clay has been dated to  $\sim\!\!35$  to  $\sim\!\!16$  ka, including the latter part of MIS 3 and the LGM. Previous work has shown that these reddish clays are marked by evidence for oxidizing conditions (reddish

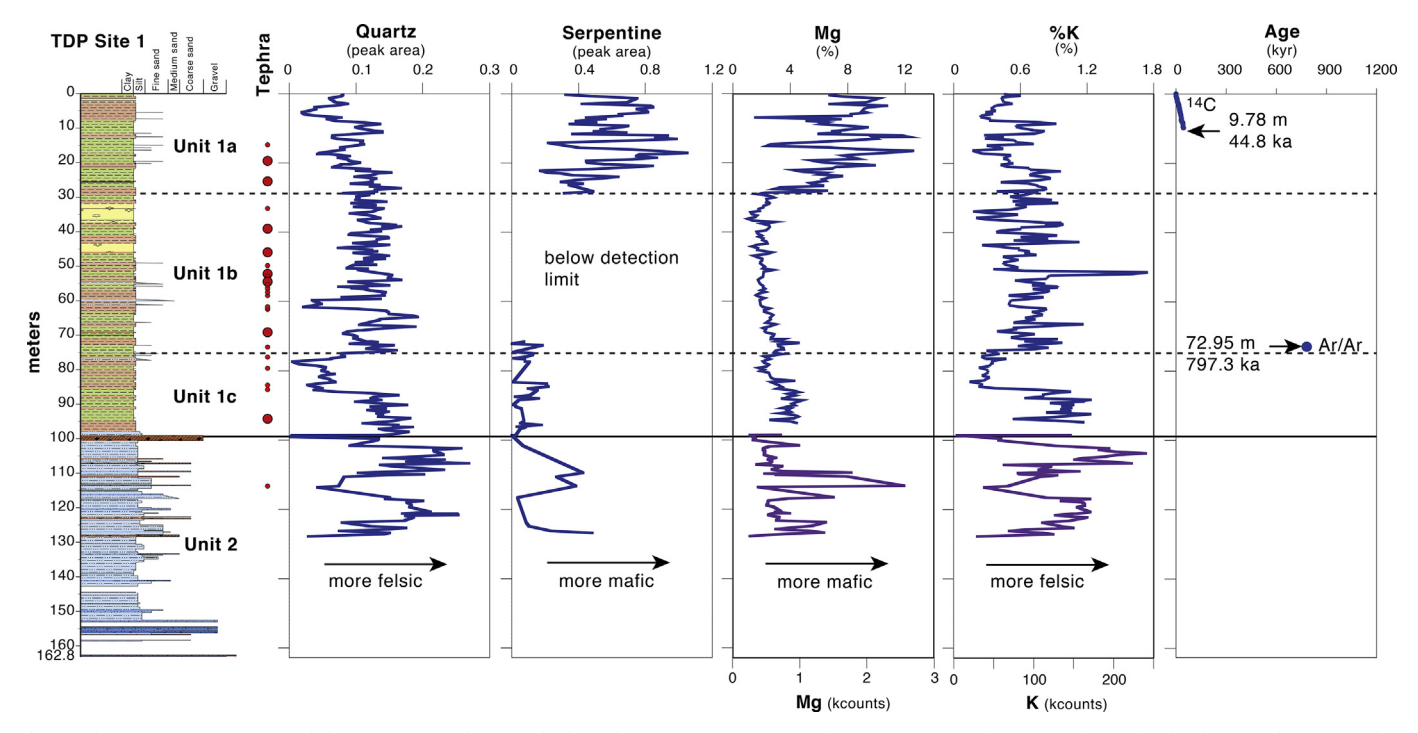


Fig. 5. The TDP Site 1 composite lithostratigraphy showing the boundaries of major stratigraphic units. Large red circles indicate the depths of tephras more than 5 cm thick; small red circles show the depths of tephras < 5 cm thick. Quartz and serpentine content (from FTIR measurements), %Mg and %K (from ICP-OES measurements), Mg and K in kilo counts (kcounts; from XRF measurements; in purple), and age determinations are shown. The key for the stratigraphic column is the same as in Fig. 4. (For interpretation of the references to color in this figure legend, the reader is referred to the web version of this article.)

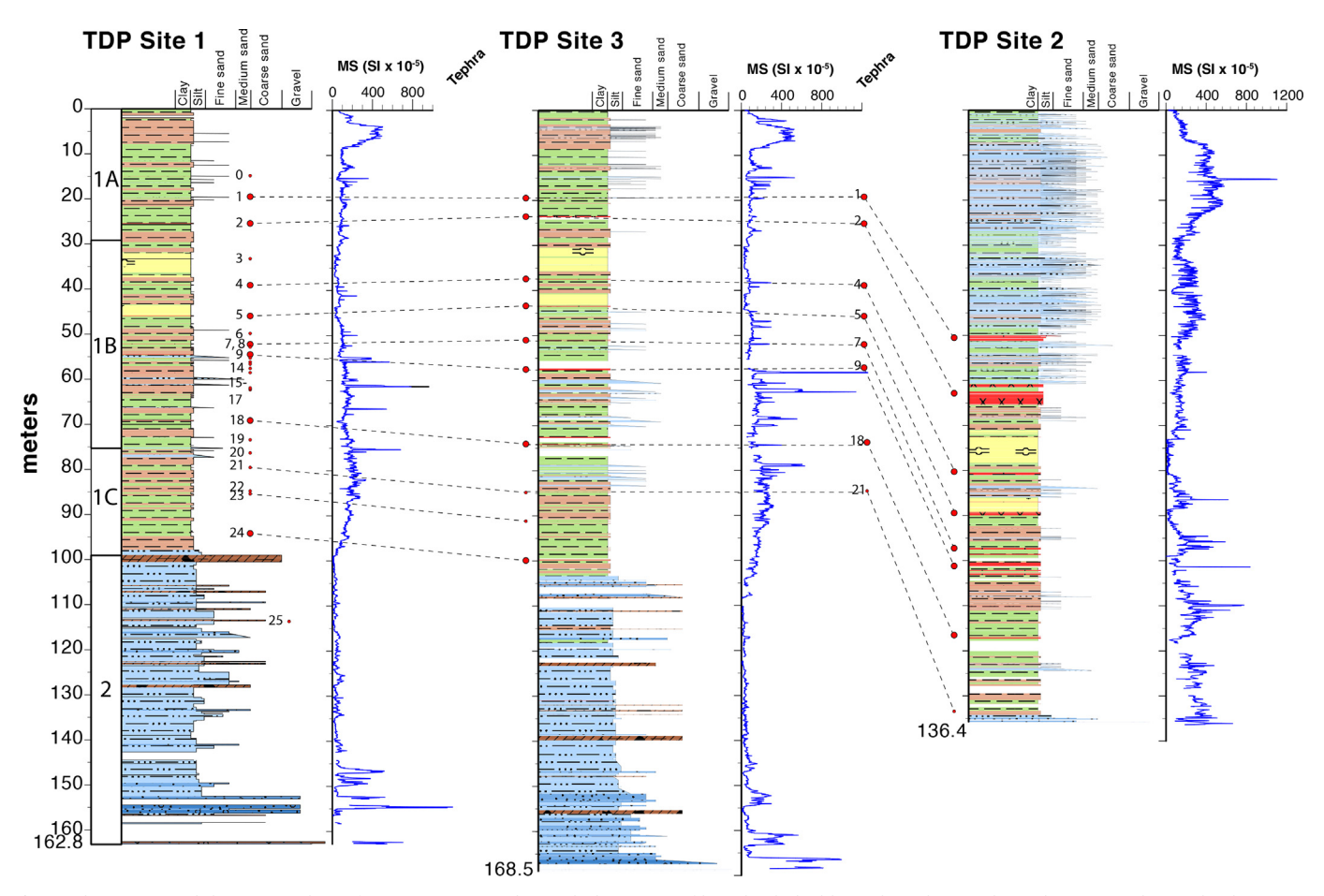


Fig. 6. The composite lithostratigraphies of TDP Sites 1, 3, and 2, with their MS profiles. The dashed lines show the correlation between tephra in the three sites, based on visual similarities and their position relative to other lithotypes. The key for the stratigraphic column is the same as in Fig. 4.

color, high Fe), but also contain abundant ferrous minerals including siderite and magnetite (e.g. Tamuntuan et al., 2015).

Alternating thinly bedded green clays and more massive to mottled sideritic clays comprise the majority of Unit 1 sediment at Site 1in Lake Towuti (Fig. 8). In addition to these lithotypes, within Unit 1 there are 24-1-20 cm thick tephra and occasional turbidites, and two ~5-m scale beds of diatomaceous ooze in Unit 1b. The reddish, sideritic clavs generally have higher MS, %Fe, % siderite, and  $\delta^{13}C_{OM}$ , and lower % TOC and TLE/TOC ratios than the green clays (Figs. 4, 8). The laminated to massive diatomaceous oozes lack siderite, have low MS and  $\delta^{13}C_{OM}$ , high TLE/TOC, and have much higher %TOC (~5%) and much lower %Fe ( $\sim$ 6%) than the other sediment types in Unit 1 (Figs. 4, 8). Turbidites and tephra were not analyzed for their geochemical properties, but have high and average MS, respectively. Tephra are most frequent between ~70 and 40 mcd, where vivianite (Fe<sub>3</sub>(PO<sub>4</sub>)<sub>2</sub>·8H<sub>2</sub>O) mottles and concretions are also common. %Fe, %Siderite, and  $\delta^{13}C_{OM}$ values are generally higher in the lowermost Unit 1c, and lower in Unit 1a.

#### 6. Discussion

# 6.1. Tectonic and geomorphic evolution of the Lake Towuti basin

The sedimentary succession in Lake Towuti in part reflects tectonically and geomorphologically driven changes in sediment source, supply, and deposition in the Lake Towuti basin over the last  $\sim 1-2$  Ma. Vertical relief and movement along the faults around and within Lake Towuti will influence source sediment supply, the lateral distribution of sediment within the lake, and the availability of accommodation space

for sediment and water. We interpret the lithified, mafic conglomerate at the base of the TDP Site 1 succession to reflect local bedrock, and the overlying reddish, dry silts to comprise a lateritic soil succession similar in composition to the laterite in today's catchment (e.g. Morlock et al., 2018). Although recovery is poor, the relatively coarse sands and gravels in the 15 m above these dry silts indicate a fluvial environment. Above this, the interbedded sands, silts, and peats suggest variable depositional environments ranging from low-energy rivers, to shallow lakes and wetlands. Similar lithologies are observed in the basal 60 m of TDP Site 3 (Fig. 6), and both correspond with the poorly stratified sediments overlying bedrock observed in our seismic reflection datasets. We therefore interpret Unit 2 to indicate a broad, low-relief setting formed during the initial stages of basin formation and subsidence.

Within Unit 2 at Site 1, we observe repeated shifts from dominantly felsic to dominantly mafic sediment sources (Fig. 5). Today, felsic sediments are sourced predominantly from the Loeha River, which drains the metasedimentary unit to the east of the lake, whereas mafic sediments are derived from much of the rest of the basin. Assuming a similar distribution of sediment sources in the past, we interpret these changes in clastic sediment source to reflect varying motion of intrabasinal faults, in particular vertical motion along the strike-slip faults that separate and bisect the central and northern basins (Fig. 2B). Today, much of the felsic sediment from the Loeha River is deposited in Lake Towuti's southern basin (Hasberg et al., 2018; Morlock et al., 2018); however, vertical motion along the fault to the south of Site 1 will influence relief within the basin and the island at the mouth of the Loeha River, and should therefore influence the distribution of the felsic sediments across the basin. In particular, increased uplift along the southern side of this fault should cause the Loeha-derived sediment to

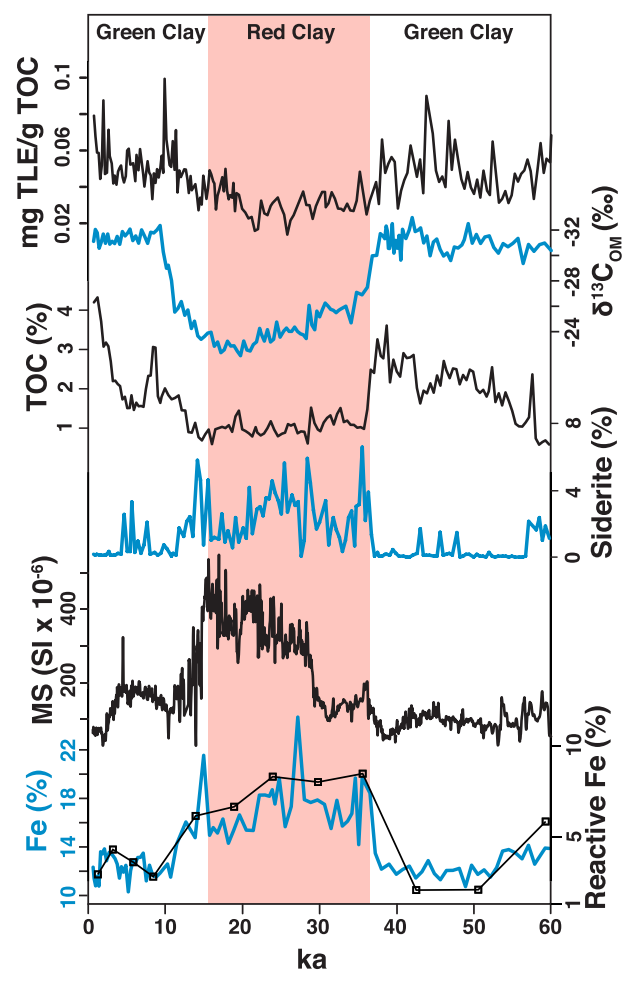


Fig. 7. %Fe, %reactive Fe, MS, %Siderite, %TOC,  $\delta^{13}C_{OM}$ , the TLE/TOC ratio from core TOW-9 plotted against age. The red shading indicates red sideritic clay lithologies, and the images at the top show red sideritic clays during MIS 2 and green clays during MIS 1 and 3. (For interpretation of the references to color in this figure legend, the reader is referred to the web version of this article.)

flow to the southern basin. Movement of the southern and northern segments of the eastern boundary fault could also influence the distribution of these sediments by controlling the relief in Lake Towuti's southern and northern basins, with accelerated subsidence in the southern basin causing increased felsic sedimentation in that part of the lake. Our data do not allow us to fully disentangle the motion along each of these faults. The different lithotypes in TDP Site 1 Unit 2 (shallow lacustrine, fluvial, peatland) could reflect climatic controls on water availability and base level, but in light of spatially variable fault motion these lithotypes may also reflect alternations in the subsidence rate at Site 1 relative to other parts of the basin. It will thus be difficult to extract a robust paleoclimate record from these sediment types in Unit 2.

The Unit 2/Unit 1 boundary marks a permanent shift to lacustrine conditions and the formation of Lake Towuti (Fig. 5). Above the peat and silt that marks this boundary at Site 1, the sediment consists of finegrained lithotypes observed through much of Unit 1, which correspond to the well-bedded, continuous sediments observed in the upper ~100 m of seismic reflection data (Fig. 2C). Although the strata above this silt are relatively thickly bedded to massive, we observe green clays containing thinly bedded (~1 cm scale) beds within 10 m of the Unit 2/Unit 1 transition (Fig. 4). Assuming anoxic bottom waters are required to preserve such thin sedimentary structures, this suggest a relatively rapid transition to deep and stratified lake environments. It is possible

that this is driven by intensified precipitation in the region; however, in light of the very humid climate today, and given that the terrestrial environments represented by Unit 2 are now overlain by  $\sim 250 \text{ m}$  of water and sediment, it seems more likely that this transition represents tectonically-driven accelerated basin subsidence. We do not observe any coarse-grained lithologies or other indications of shallow-water deposition or aerial exposure in Unit 1, indicating permanent lacustrine conditions above the Unit 2/Unit 1 transition. Oscillations between more felsic and ultramafic sediments, indicating variable fault motion, continue through the lower 25 m, until the Unit 1c/1b transition (Fig. 5). Assuming that climate change would cause relatively uniform changes in erosion rates, regardless of lithotype, these shifts in sediment source likely indicate the continued influence of tectonically-driven changes in basin morphology and catchment hydrology on sediment sources to the site. Above this, Units 1b and 1a suggest a relatively stable tectonic setting with more gradual subsidence rates in a lake similar to the present day.

Although there is considerable uncertainty in our chronology, and sedimentation rates likely varied as the basin subsided near the Unit 1/ Unit 2 boundary, using the age of 797 ka at 72.95 mcd, and a sedimentation rate of 0.092 m/kyr (based on linear interpolation from the core top to the 40Ar/39Ar age), we estimate the age of formation of a permanent Lake Towuti at ~1 Ma. This age is highly uncertain, as it relies on extrapolation of sedimentation rates across very different sediment types. However, this age is broadly consistent with previous estimates of the age of formation of the Malili Lake basins (which would include sediments in Unit 2) of 1.5-2 Ma (Ahmad, 1977). It is important to note that this does not imply that Lake Towuti as it exists today formed instantaneously across the entire lake basin. Indeed, based on our tephrostratigraphic correlations between Sites 1 and 2, the lowermost ~18 m of Unit 1 at Site 1 is missing at Site 2 indicating that the Unit 1/Unit 2 boundary, and the transition to permanent lacustrine conditions, occurred later at Site 2 than at Site 1. Thus, the northernmost basin of the lake is considerably younger than the central part of the northern basin, implying very rapid movement of the faults in the northern part of the lake during the mid- to late Pleistocene to produce what is now the deepest part of the lake.

Although Units 1b and 1a indicate relatively stable lacustrine conditions, there are clear signals of geomorphic reorganization within Unit 1. The Unit 1b/1a boundary is marked by a prominent rise in %Mg and serpentine (Fig. 5), closely followed by frequent turbidite deposition at Site 2. In the modern lake, the Mahalona River is the primary source of Mg- and serpentine-rich sediments to Towuti's northern basin (Goudge et al., 2017; Hasberg et al., 2018; Morlock et al., 2018). The onset of rapid sedimentation rates and turbidite deposition at Site 2, which sits near the eastern edge of the Mahalona River delta, further suggest this transition is caused by the reorganization of that river. Today, the Mahalona River drains a vast area north of Lake Towuti, including Lakes Matano and Mahalona, and accounts for ~35% of the water input to Lake Towuti. Yet Lakes Matano and Mahalona, which sit less than 10 km upstream, must trap most of the sediment from these northern catchments. The shift in sediment composition at the Unit 1b/ 1a transition in Site 1 thus reflects the connection of the Lampenisu and Mahalona Rivers between Lakes Mahalona and Towuti, rather than connection of Lake Towuti to the upstream lakes. This connection could occur due to backcutting of the Mahalona and capture of the Lampenisu River, and/or infilling of Lake Mahalona and the sedimentary plain to its east causing southward migration of the Lampenisu River's connection to the Mahalona. The Mahalona River supplies ~37% of Lake Towuti's water inputs today, and we do not observe evidence for a large increase in lake level at the Unit 1b/1a transition. Therefore, we do not interpret this transition to reflect the establishment of the connections between the Malili Lakes (i.e. the Mahalona River).

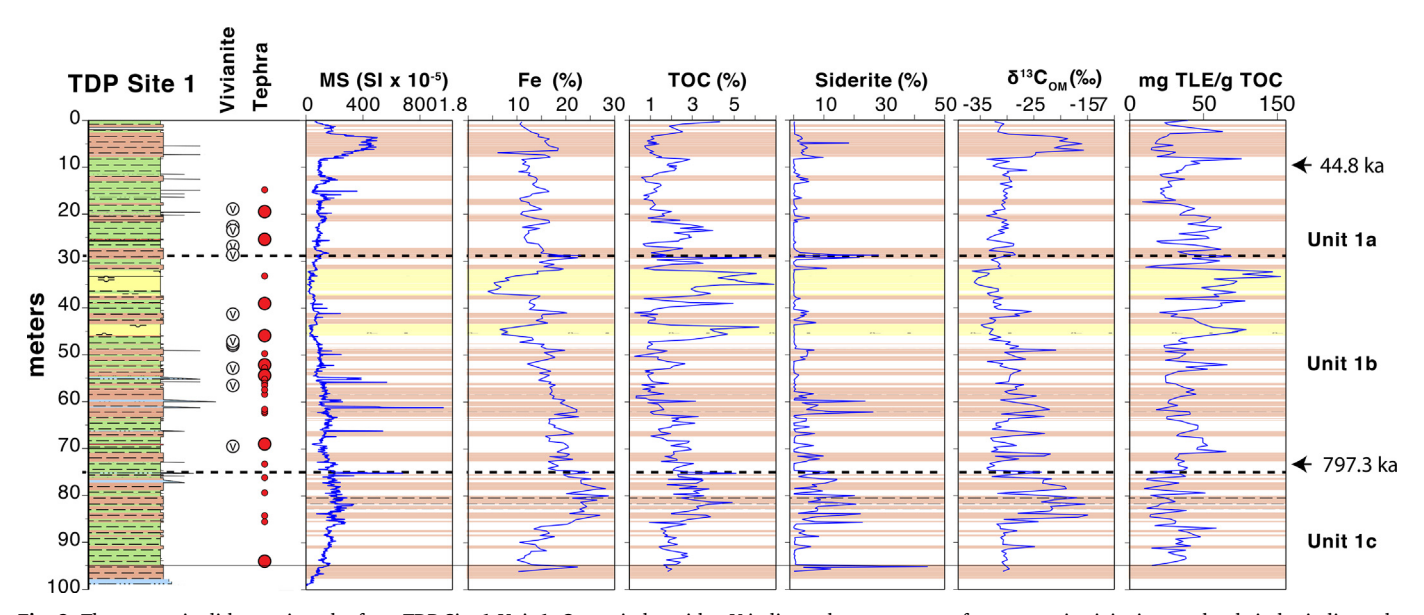


Fig. 8. The composite lithostratigraphy from TDP Site 1 Unit 1. Open circles with a V indicate the occurrence of macroscopic vivianites, and red circles indicate the presence of macroscopic tephra (as int Fig. 5). The MS, %Fe (from ICP-OES), %TOC, %Siderite, the  $\delta^{13}C_{OM}$ , and the TLE/TOC ratio are shown. Red shading indicates red sideritic clay; yellow shading indicates diatom oozes. (For interpretation of the references to color in this figure legend, the reader is referred to the web version of this article.)

#### 6.2. Biogeochemical evolution of Lake Towuti during the Pleistocene

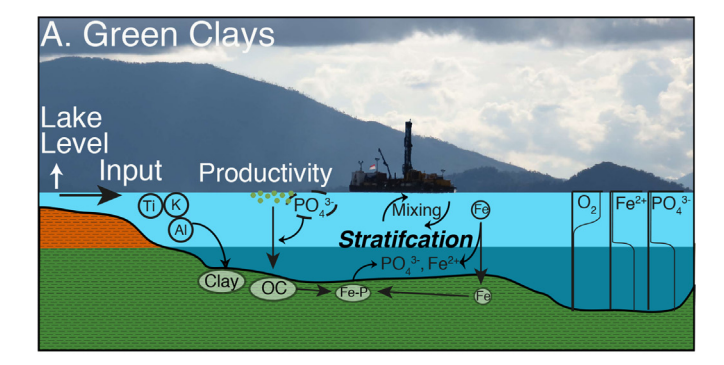
Based on the data from TOW-9, we posit that changes in the iron mineralogy, carbon concentrations, and other biogeochemical proxies in Lake Towuti are caused by climate-driven changes in lake mixing and oxygenation. Today, the relatively warm, humid conditions promote water column stratification in Lake Towuti, with anoxia and high dissolved Fe concentrations below ~100 m (Costa et al., 2015; Vuillemin et al., 2016). Despite the reducing conditions in the water column, reduced Fe minerals including siderite, vivianite, and magnetite are absent or at low concentrations in late Holocene sediment (Fig. 7). Siderite is generally absent from catchment soils, indicating that its presence is not related to supply from the catchment (Morlock et al., 2018; Sheppard et al., 2019). Thus, the Fe mineralogy of these sediments does not directly reflect water column oxygenation nor detrital mineral input, suggesting these minerals instead form authigenically. In contrast to the modern sediments, sediments deposited during the LGM in TOW-9 contain relatively abundant siderite and magnetite, despite a reddish color suggesting oxidizing conditions. During this interval, Lake Towuti experienced increased input of OM from plants using the C<sub>4</sub> photosynthetic pathway, a ~ 10-30 m decline in lake levels, and reduced water column anoxia, all consistent with a drier climate (Costa et al., 2015; Russell et al., 2014; Vogel et al., 2015). We suggest that this cooler, drier climate promoted lake mixing, bottom water oxygenation, and increased flux of reactive ferric iron to the sediment. This ferric iron promoted reductive iron dissolution and in situ formation of siderite and magnetite.

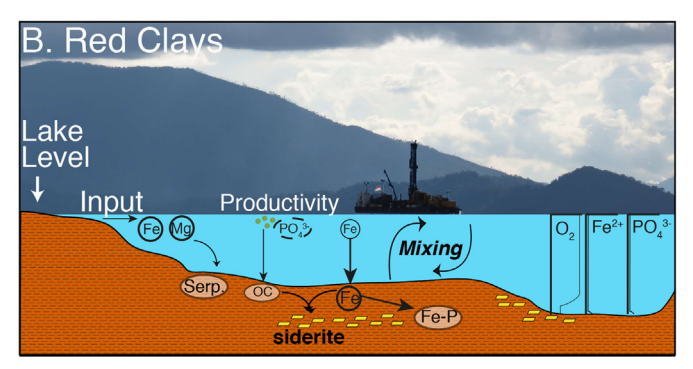
A cooler, drier climate, especially with an enhanced dry season, will promote more frequent water column mixing and oxygenation of the lake floor. This increases the flux of reactive iron to the sediment (Fig. 7, 9A, B), promoting dissimilatory iron reduction (DIR), known to occur at shallow water depth in sediments in modern Lake Towuti (Vuillemin et al., 2016). The pore water alkalinity in Lake Towuti's sediment is relatively high (> 2 mM), likely due to a variety of microbial metabolic processes and pore fluid migration (Vuillemin et al., 2019), which, together with the near absence of siderite in green clays, further highlights the importance of reactive iron and DIR in the red clays for siderite formation. DIR may also explain elevated MS observed in the reddish clays of TOW-9 and in some reddish clays in Unit 1. Indeed, previous work has shown that much of the observed magnetite

is composed of very fine-grained, super-paramagnetic grains which often form as a consequence of DIR (Tamuntuan et al., 2015). Siderite formation at Lake Towuti has been suggested to occur through a series of unstable intermediary minerals, from iron oxyhydroxides to green rust to siderite (Vuillemin et al., 2019). Our analyses show that the ultimate trigger for these changes is enhanced lake mixing and ensuing burial of reactive iron under a cooler and drier climate.

In addition to changes in lake mixing, variable lake levels could also contribute to the formation of the reddish, sideritic clays. Vogel et al. (2015) estimated a  $\sim$  10-30 m reduction in Lake Towuti's water level during the LGM, shifting Lake Towuti to closed-basin conditions. The reduction in water levels would move the oxygenated mixed layer at the surface closer to the lake floor; however, even a ~ 30 m lake level decline cannot explain the redox changes observed in the sediment, as the anoxic hypolimnion today is ~50 m deep. Moreover, we observe red, sideritic clay in Site 2 (interbedded with numerous turbidites, Fig. 6), located at 200 m water depth, further suggesting much deeper water column mixing than is common today. The transition to closedbasin conditions may enhance the water column alkalinity through evaporative concentration of dissolved carbonate and bicarbonate, promoting siderite formation in shallow sediments where pore fluids interact with the overlying surface water. Indeed, siderite is not present in shallow sediment under oxygenated water in the modern lake (Sheppard et al., 2019), suggesting bottom water oxygenation alone will not trigger siderite formation. However, %Fe in shallow sediments in the modern lake are also lower than in the red clays in TOW-9 and Unit 1 sediments (Hasberg et al., 2018; Morlock et al., 2018; Sheppard et al., 2019). Thus a change in lake mixing dynamics driven by changes in lake surface temperature are critical to the red clay/green clay transition.

Changes in lake mixing and iron biogeochemistry in Lake Towuti were coupled to large changes in the lake's carbon cycle, marked by changes in TOC,  $\delta^{13}C_{OM}$ , and TLE/TOC ratios. Today, TOC averages  $\sim\!4\%$  across most of the lake and C/N averages  $\sim\!13$  suggest a mix of degraded aquatic and terrestrial OM (Hasberg et al., 2018). The  $\delta^{13}C_{OM}$  averages about -35%, likely reflecting isotopically depleted inputs from rainforest vegetation and low aquatic primary productivity (Hasberg et al., 2018). We interpret the more enriched  $\delta^{13}C_{OM}$  associated with red clays (Figs. 7, 8) to multiple causes, including changes in lake primary productivity, OM sources, and OM respiration in the





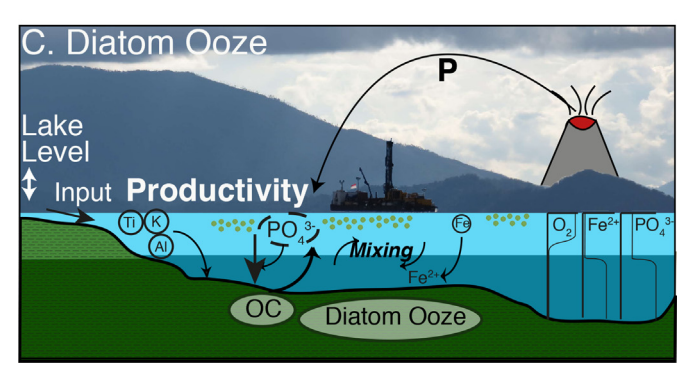


**Fig. 9.** Schematic figures indicating inferred changes in lake level, water column mixing, oxygenation, nutrient concentrations, and biogeochemical cycling resulting in the formation of green clays, red clays, and diatomaceous oozes in Lake Towuti. (For interpretation of the references to color in this figure legend, the reader is referred to the web version of this article.)

water column and sediment (Fig. 9B; e.g. Meyers and Teranes, 2001). The modern lake is ultraoligotrophic, marked by extremely low phosphate concentrations and biomass (Sabo et al., 2008; Bramburger et al., 2008), likely due to P trapping by iron oxyhydroxides in the sediment (Crowe et al., 2008b), yet some P might slowly diffuse from deeper sediment under an anoxic water column into the overlying water to support primary production. The increased concentrations of reactive iron oxyhydroxides in the red clays should further enhance P trapping in the sediment, particularly in this low sulfate lake (Caraco et al., 1989), thereby reducing P recycling and lake primary productivity and contributing to low %TOC (Fig. 9B). Lower primary productivity, enhanced deep-water oxygenation, and higher rates of dissimilatory iron reduction likely all contribute to the presence of low quality OM. The controls on the  $\delta^{13}C_{OM}$  are more difficult to determine, but in the TOW-9 record the LGM is marked by enriched  $\delta^{13}\text{C}$  of terrestrial leaf waxes, indicating increased fluxes of terrestrial C<sub>4</sub> biomass to the lake (Russell et al., 2014). The bulk OM should consist of a mixture of terrestrial and aquatic biomass, but lower rates of primary production combined with increased inputs of C4 vegetation to the lake could explain elevated δ<sup>13</sup>C<sub>OM</sub> signatures. The increase in terrestrial relative to aquatic carbon

would further contribute to the reduction in OM quality (e.g. Meyers and Teranes, 2001; Talbot et al., 2006). We thus infer that the red /green clay alternations in Unit 1 most likely reflect orbital-scale alternations between cooler, drier conditions that promote lower lake levels and lake mixing, and warmer, wetter climates that promote a more productive, stratified lake.

We also observe long-term, secular changes in %Fe and %Siderite in Unit 1, from generally higher values in Unit 1c to lower concentrations at the top of the succession. We suggest that these changes are driven by the tectonic evolution of the lake basin, and in particular a gradual increase in accommodation space, and its influence on lake water depth, water column oxygenation, and diagenetic growth of Fe minerals. A shallower lake during the initial stages of Lake Towuti's formation should favor the burial of reactive iron oxyhydroxides, favoring high %Fe and eventual formation of siderite. Siderite in Unit 1c and lower 1b often consists of much coarser-grained siderite than observed in Unit 1a, including large mottles and concretions, suggesting continued siderite growth in the sediments (though not in green clays). %TOC values are generally higher in Unit 1c, suggesting the lake carbon and iron biogeochemical cycles differed during this interval. This could reflect multiple processes, including enhanced primary production in a smaller, shallower Lake Towuti driven by benthic lakewide primary production, increased inputs of nutrients relative to the lake volume, or more efficient internal loading of nutrients from the sediment due to the shallower water column.

Although the red clay/green clay lithotypes record clear changes in the lacustrine iron and carbon cycles, the largest changes in carbon cycling occur during the deposition of the diatomaceous oozes (Fig. 8). The diatoms consist largely of species from the genus *Aulacoseira* that, together with the other sedimentary variables, suggest a mesotrophic lake with abundant diatoms in the phytoplankton (Gasse, 1986). This contrasts enormously with the present-day ultraoligotrophic lake that lacks planktonic diatoms (Bramburger et al., 2008). The presence of these diatom oozes thus reflects very large changes in nutrient loading in Lake Towuti. Although the bedrock is generally ultramafic, Si concentrations are high enough in the modern lake (9 mg/L; Friese et al., in review) to support diatom production. Rather, phosphorus concentrations are well below detection limits indicating a strongly P-limited ecosystem, and suggesting that increased diatom production must reflect higher rates of P-loading.

We suggest that tephra are at least partially, if not largely, responsible for increased P inputs and the formation of diatomaceous oozes, based upon the co-occurrence of the diatom oozes, frequent tephras, and vivianite (a hydrated iron phosphate mineral) between 60 and 30 mcd (Fig. 8). Not all tephra are directly associated with vivianite, and although the lowermost diatom ooze (43–46 mcd) directly overlies a thick tephra (46 mcd) near multiple vivianite nodules, the upper diatom ooze ( $\sim$ 37 to 32 mcd) has no immediately preceding tephra, and instead sits > 2 m above a thick tephra at  $\sim$ 39 mcd. This could indicate that the response of the lake ecosystem may depend not only on tephra depositional rate and composition, but also on other environmental factors, such as lake mixing. Nevertheless, the association of diatomaceous sediments and tephra horizons in this particular interval of core suggests they are related.

Increased primary productivity in response to tephra input have been previously observed in tropical paleolimnological studies, where P and Si leached from tephra in the lake stimulates production by diatoms (Barker et al., 2000; Hickman and Reasoner, 1994). These responses have generally been short, in contrast to the prolonged and potentially delayed responses in Lake Towuti. We therefore suggest that increased diatom production depends less on deposition of tephra-bound P directly into the lake than on accumulation and subsequent weathering of tephra in the catchment. The peridotites in Towuti's catchment have P concentrations of 0.02% (Monnier et al., 1995) and are very deeply weathered. Given these extremely low P concentrations of Towuti's catchment bedrock, external P subsidies must be essential to stimulate

relatively high productivity, and tephra and volcanic aerosols are the most likely source. The P content of Indonesian volcanic glasses are variable but average about 0.1% (Ninkovich, 1979). Assuming a density of ~2400 kg/m³(Wilson et al., 2011), a 10 cm thick tephra would deposit ~240 g P/m<sup>2</sup> onto the catchment, equivalent to 480 g P/m<sup>2</sup> of lake surface area. If that P is weathered into the lake's photic zone over 10,000 years, it yields an average concentration of 5 μg P/L, suggesting a weakly mesotrophic lake. This concentration is too low to trigger a sustained shift to mesotrophic conditions, and it is also likely that in the tropical climate surrounding Lake Towuti the tephra weathers much more quickly than 10,000 years. This suggests that individual tephra inputs may not fully explain the diatomaceous oozes. Rather, P supplements to Lake Towuti can derive from the accumulation and weathering of multiple tephra deposits through time, as well as limnological changes that promote more efficient recycling of P within the lake.

Thus we suggest that inputs of P from tephra must be coupled with changes in lake mixing and or water depth to promote mesotrophic conditions in the lake. P is intensely recycled in lake ecosystems, such that internal loading from the sediment often eclipses the catchment as the dominant source of P to the water column on an annual basis, particularly in tropical lakes (Kilham and Kilham, 1990). The laminations in sections of these oozes suggest seasonal mixing of at least part of the water column that could bring P from depth to the photic zone, whereas the low %Fe, high %TOC values, and relatively well-preserved OM (high TLE/TOC) suggest water anoxia that would promote P release to the water column. It is likely that the lake was slightly shallower at this time given gradual subsidence of the basin. All of these conditions would promote more efficient internal recycling of P to the photic zone, with anoxia and low Fe promoting P release into the water column, and seasonal mixing in a shallow lake promoting transfer to the photic zone (Fig. 9C). This result has important implications for management of the modern lake, given rapid land clearance over the last decade for fertilizer-dependent agriculture. In particular, our results suggest the potential for rapid, long-term switches in Lake Towuti's trophic state in response to small perturbations in nutrient input, suggesting that nutrient loading to the lake should be carefully monitored and managed.

#### 6.3. Implications for paleoclimate and biological endemism in Lake Towuti

Although we see no evidence for complete lake desiccation as witnessed in other parts of the tropics, such as East Africa (Gasse, 2000; Johnson et al., 1996; Scholz and Rosendhal, 1988), Lake Towuti has experienced large changes in precipitation during the Pleistocene. Because nearly 75% of the modern water inputs are lost to outflow, large precipitation, evaporation, and catchment evapotranspiration changes are required to induce lowstands in Lake Towuti. This is highlighted by a lake level decline of 3 m and a transition to nearly closed-basin conditions in response to a  $\sim$  50% reduction in rainfall during the 1997-1998 El Niño event (Tauhid and Arifian, 2000). This, in turn, requires very large reductions in wet season precipitation, given the importance of the wet season to Lake Towuti's water budget. The most recent of these events, during the LGM, is associated with deeper water column mixing, suggesting a longer and/or stronger dry season than occurs today. Thus, the frequent red sideritic clays suggest repeated intervals of considerably drier wet and dry season conditions in Lake Towuti's past, in contrast to other regions in Indonesia where the LGM may have been associated with pronounced seasonal contrasts in rainfall (Ruan et al., 2019). This also stands in contrast to models that invoke relatively modest changes in precipitation during the late Quaternary to support the development of Indonesian rainforests (Cannon et al., 2009).

Aside from the LGM, the timing of red clay deposition in Unit 1 is uncertain, but red clays and turbidites coincide at all three sites during several events in the upper  $\sim\!80$  m, suggesting repeated changes in lake mixing and water level during the mid- to late Pleistocene. Our age

model severely limits our ability to assign these features to particular orbital-scale forcings; however, we observe  $\sim \! 14$  siderite beds at least 1 m thick from the  $\sim \! 797$  ka tephra to the top of the core, suggesting that climate variations cannot be attributed solely to  $\sim \! 100$  kyr glacial-interglacial cycles nor orbital precession. This is in keeping with results from the region suggesting both low latitude insolation as well as high-latitude ice volume influence on IPWP hydrology (Carolin et al., 2016; DiNezio and Tierney, 2013; Krause et al., 2019; Russell et al., 2014). Future work using a more refined age model and sensitive climate proxies will further refine this climate history.

Our record holds important implications for the evolution of Lake Towuti's extraordinary fauna, Molecular-clock estimates suggest that Lake Towuti's telmatherinid fishes initially diverged from a riverine ancestor at about 0.7 Ma (0.18-1.37 Ma), when the clock is calibrated using geological data from New Guinea (Stelbrink et al., 2014). This timing is similar to, though slightly younger than, our estimated age of Lake Towuti, suggesting either that the fishes did not colonize the lake for several hundred thousand years after its formation (which seems unlikely) or that the clock could be further refined as indicated by the comparatively large error bars (0.18-1.37 Ma). The genetic data also suggest that these ancestors likely colonized Lake Towuti from the Mahalona River, in support of our inference of the Mahalona River's existence during the mid-Pleistocene. The present data are thus compatible with a model of allopatric speciation in the Malili Lakes as reflected by their endemism. This could be related to physical dispersal limits imposed by the regional rivers, such as stretches of rapids or lack of suitable habitat in the rivers between the lakes. However, interestingly, dispersal limits seem to also exist today for highly mobile taxa such as zooplankton populations, suggesting between-lake dispersal limits could arise from differences in lake chemistry, such as metal concentrations and toxicological barriers, rather than physical barriers (e.g. Vaillant et al., 2011). With the exception of the diatomaceous oozes, Lake Towuti appears to have maintained generally low primary productivity through most of its history. The evolution of feeding specializations in fish, gastropods, shrimps, and other taxa to leverage resources in a variety of benthic substrates and habitats is in keeping with the extreme food scarcity observed in the lake in the present and through much of its past.

#### 7. Conclusions

Sedimentological and geochemical analyses of drill cores from Lake Towuti show that the lake formed during a phase of rapid tectonic subsidence at ~1 Ma from a landscape characterized by active river channels, shallow lakes and swamps. The sediment succession deposited during the last 1 Myr is characterized by alternations of green organic rich and red sideritic clay beds that reflect repeated shifts between warm, wet and cooler, drier climates, respectively, likely driven by both orbital-scale changes in insolation and continental ice volume. Two meters-thick beds of planktonic diatomaceous oozes reflect phases of substantially increased primary productivity, likely driven by inputs of P from tephra and changes in internal P cycling. Our estimate that a permanent lake formed at ~1 Ma agrees with molecular-clock estimates of ~0.7 Ma (0.18-1.37 Ma) for the divergence of Lake Towuti's Telmatherinid fishes from a riverine ancestor and are compatible with an evolutionary model in which Lake Towuti's endemic fauna is a result of geographic speciation in the Malili Lakes. More detailed chronological constraints and refined climate and environmental proxy datasets are currently in preparation and will help to paint a more detailed history of the region's climate and environmental history.

# **Declaration of Competing Interest**

The authors declare that they have no known competing financial interests or personal relationships that could have appeared to

influence the work reported in this paper.

#### Acknowledgements

This research was carried out with partial support from the International Continental Scientific Drilling Program (ICDP), the U.S. National Science Foundation (NSF), the German Research Foundation (DFG) the Swiss National Science Foundation (SNSF), PT Vale Indonesia, the Ministry of Research, Education, and Higher Technology of Indonesia (RISTEK), Brown University, the GFZ German Research Centre for Geosciences, the Natural Sciences and Engineering Research Council of Canada (NSERC), and Genome British Columbia. We thank PT Vale Indonesia, the US Continental Scientific Drilling and Coordination Office, and US National Lacustrine Core Repository, and DOSECC Exploration Services for logistical support. The research was carried out with permissions from RISTEK, the Ministry of Trade of the Republic of Indonesia, the Natural Resources Conservation Center (BKSDA), and the Government of Luwu Timur of Sulawesi. Cores and data are archived at the National Lacustrine Core Repository, USA, and data are available at NOAA's World Data Center for Paleoclimatology at the time of publication.

#### Appendix A. Supplementary data

Supplementary data to this article can be found online at https://doi.org/10.1016/j.palaeo.2020.109905.

#### References

- Adler, R., Wang, J.-J., Sapiano, M., Huffman, G., Chiu, L., Xie, P.-P., Ferraro, R., Schneider, U., Becker, A., Bolvin, D., Nelkin, E., Gu, G., Program, N.C., 2016. Global Precipitation Climatology Project (GPCP) climate Data Record (CDR). Version 2, 3 (Monthly), in: doi:10.7289/V56971M6, N.C.f.E.I. (Ed.).
- Ahmad, W., 1977. Geology along the Matano Fault Zone, East Sulawesi, Indonesia, Regional Conference on the Geology and Mineral Resources of Southeast Asia. Jakarta, Indonesia.
- Aldrian, E., Susanto, R.D., 2003. Identification of three dominant rainfall regions within Indonesia and their relationship to sea surface temperature. Inter. Jour. Climat. 23, 1435–1452.
- Ayliffe, L.K., Gagan, M.K., Zhao, J.-X., Drysdale, R.N., Hellstrom, J.C., Hantoro, W.S., Griffiths, M.L., Scott-Gagan, H., St. Pierre, E., Cowley, J.A., Suwargadi, B.W., 2013. Rapid interhemispheric climate links via the Australasian monsoon during the last delgaciation. Nat. Commun. 4, 2908.
- Barker, P., Telford, R.J., Merdaci, O., Williamson, D., Taieb, M., Vincens, A., Gibert, E., 2000. The sensitivity of a Tanzanian crater lake to catastrophic tephra input and four millennia of climate change. Holocene 10, 303–310.
- Bellier, O., Sebrier, M., Seward, D., Beaudouin, T., Villeneuve, M., Putranto, E., 2006. Fission track and fault kinematics analyses for new insight into the late Cenozoic tectonic regime changes in West-Central Sulawesi (Indonesia). Tectonophysics 413, 201–220.
- Bramburger, A.J., Haffner, G.D., Hamilton, P.B., Hinz, F., Hehanussa, P.E., 2006. An examination of species within the genus Surirella from the Mailii Lakes, Sulawesi Island, Indonesia. Diatom Research 21, 1–56.
- Bramburger, A.J., Hamilton, P.B., Hehanussa, P.E., Haffner, G.D., 2008. Processes regulating the community composition and relative abundance of taxa in the diatom communities of the Malili Lakes, Sulawesi Island, Indonesia. Hydrobiologia 615, 215–224.
- Brooks, J.L., 1950. Speciation in ancient lakes. Q. Rev. Biol. 25, 131-176.
- Cane, M.A., 2005. The evolution of El Nino, past and future. Earth Planet. Sci. Lett. 230, 227–240.
- Cannon, C.H., Morley, R.J., Bush, A.B.G., 2009. The current refugial rainforests of Sundaland are unprepresentative of their biogeographic past and highly vulnerable to disturbance. Proc. Natl. Acad. Sci. 106, 11188–11193.
- Caraco, N.F., Cole, J., Likens, G.E., 1989. Evidence for sulphate-controlled phosphorus release from sediments of aquatic systems. Nature 341, 316–318.
- Carolin, S.A., Cobb, K.M., Lynch-Stieglitz, J., Moerman, J., Partin, J.W., Lejau, S., Malang, J., Clark, B., Tuen, A.A., Adkins, J., 2016. Northern Borneo stalagmite records reveal West Pacific hydroclimate across MIS 5 and 6. Earth Planet. Sci. Lett. 439, 182–193.
- Chiang, J.C.H., 2009. The tropics in paleoclimate. Annu. Rev. Earth Planet. Sci. 37, 20.21–20.35.
- Clement, A.C., Cane, M.A., Seager, R., 2001. An orbitally-driven tropical source for abrupt climate change. J. Clim. 14, 2369–2375.
- Costa, K., Russell, J.M., Vogel, H., Bijaksana, S., 2015. Hydrologial connectivity and mixing of Lake Towuti, Indonesia in response to paleoclimatic change over the last 60,000 years. Palaeogeogr. Palaeoclimatol. Palaeoecol. 417, 467–475.
- Crowe, S.A., Jones, C.A., Katsev, S., Sturm, A., O'Neill, A.H., Haffner, G.D., Canfield, D., Sundby, B., Mucci, A., Fowle, D.A., 2008a. Photoferrotrophs thrive in an ancient

- ocean analogue. Proc. Natl. Acad. Sci. 105, 15938-15943.
- Crowe, S.A., O'Neill, A.H., Katsev, S., Hehanussa, P.E., Haffner, G.D., Sundby, B., Mucci, A., Fowle, D.A., 2008b. The biogeochemistry of tropical lakes: a case study from Lake Matano. Indonesia. Limnol. Oceanog. 53, 319–331.
- Crowe, S.A., Paris, G., Katsev, S., Jones, C., Kim, S.-T., Zerkle, A.L., Nomosatryo, S., Fowle, D.A., Adkins, J.F., Sessions, A.L., Farquhar, J., Canfield, D., 2014. Sulfate was a trace constituent of Archean seawater. Science 346, 735–739.
- Deino, A.L., Behrensmeyer, A.K., Brooks, A.S., Yellen, J.E., Sharp, W.D., Potts, R., 2018. Chronology of the Acheulean to Middle Stone Age transition in eastern Africa. Science 360, 95–98.
- DiNezio, P.N., Tierney, J.E., 2013. The effect of sea level on glacial Indo-Pacific climate. Nat. Geosci. 6, 485–491.
- Fritz, S.C., Baker, P.A., Seltzer, G.O., Ballantyne, A., Tapia, P.M., Cheng, H., Edwards, R.L., 2007. Quaternary glaciation and hydrologic variation in the South American tropics as reconstructed from the Lake Titicaca drilling project. Quat. Res. 68, 410–420.
- Gasse, F., 1986. East African Diatoms: Taxonomy, Ecological Distribution. J. Cramer, Berlin.
- Gasse, F., 2000. Hydrological changes in the African tropics since the Last Glacial Maximum. Quat. Sci. Rev. 19, 189–211.
- Goudge, T.A., Russell, J.M., Mustard, J.F., Head, J.W., Bijaksana, S., 2017. A 40,000 year record of clay mineralogy at Lake Towuti, Indonesia: paleoclimate reconstruction from reflectance spectroscopy and perspectives on paleolakes on Mars. Geol. Soc. Am. Bull. 129, 806–819.
- Haffner, G.D., Hehanussa, P.E., Hartoto, D., 2001. The biology and physical processes of large lakes of Indonesia: Lakes Matano and Towuti. In: Munawar, M., Hecky, R.E. (Eds.), The Great Lakes of the World (GLOW): Food-Web, Health, and Integrity. Blackhuys, Leiden, The Netherlands, pp. 129–155.
- Hall, R., 2017. Southeast Asia: new views of the geology of the Malay Archipelago. Annu. Rev. Earth Planet. Sci. 45, 331–358.
- Hall, R., Wilson, M.E.J., 2000. Neogene sutures in eastern Indonesia. J. Asian Earth Sci. 18, 781–808.
- Hamilton, W., 1979. Tectonics of the Indonesia Region, United States Geological Survey Professional Paper, P. 345 pp.
- Hamilton, W.B., 1988. Plate tectonics and island arcs. Geol. Soc. Am. Bull. 100 1503–1327.
- Hasberg, A.K.M., Bijaksana, S., Just, J., Melles, M., Morlock, M., Opitz, S., Russell, J.M., Vogel, H., Wennrich, V., 2018. Modern sedimentation processes in Lake Towuti, Indonesia, revealed by the composition of surface sediments. Sedimentology 66, 675–698.
- Hendon, H.H., 2003. Indonesian rainfall variability: impacts of ENSO and local air-sea interaction. J. Clim. 16. 1775–1790.
- Herder, F., Nolte, A.W., Pfänder, J., Schwarzer, J., Hadiaty, R.K., Schliewen, U.K., 2006. Adaptive radiation and hybridization in Wallace's dreamponds: evidence from sailfin silversides in the Malili lakes of Sulawesi. Proceedings of the Royal Society of London B Biological Sciences 273, 2209–2217.
- Hickman, M., Reasoner, M.A., 1994. Diatom responses to late Quaternary vegetation and climate change, and to deposition of two tephras in an alpine and sub-alpine lake in Yoho National Park, British Columbia. Jour. Paleolim. 11, 173–188.
- Johnson, T.C., Scholz, C., Talbot, M.R., Kelts, K.R., Ricketts, R.D., Ngobi, G., Beuning, K.R.M., McGill, J.W., 1996. Late Pleistocene desiccation of Lake Victoria and rapid evolution of cichlid fishes. Science 276, 786–788.
- Johnson, T.C., Werne, J.P., Brown, E.T., Abbott, A., Berke, M.A., Steinman, B.A., Halbur, J., Contreras, S., Grosshuech, S., Deino, A.L., Lyons, R.P., Scholz, C., Schouten, S., Sinninghe Damsté, J.S., 2016. A progressively wetter climate in southern East Africa over the past 1.3 million years. Nature 537, 220–224.
- Kadarusman, A., Miyashita, S., Maruyama, S., Parkinson, C.D., Ishikawa, A., 2004.Petrology, geochemistry, and paleogeographic reconstruction of the East Sulawesi ophiolite, Indonesia. Tectonophysics 392, 55–83.
- Kilham, P., Kilham, S.S., 1990. Endless summer: Internal loading processes dominate nutrient cycling in tropical lakes. Freshw. Biol. 23, 379–389.
- Konecky, B.L., Russell, J.M., Bijaksana, S., 2016. Glacial aridity in Central Indonesia coeval with intensified monsoon circulation. Earth Planet. Sci. Lett. 437, 15–24.
- Krause, C.E., Gagan, M.K., Dunbar, G.B., Hantoro, W.S., Hellstrom, J.C., Cheng, H., Edwards, R.L., Suwargadi, B.W., Abram, N.J., Rifai, H., 2019. Spatio-temporal evolution of Australasian monsoon hydroclimate over the last 40,000 years. Earth Planet. Sci. Lett. 513. 103–112.
- Lehmusluoto, P., Machbub, B., Terangna, N., Rusmiputro, S., Achmad, F., Boer, L., Brahmana, S.S., Priadi, B., Setiadji, B., Sayuman, O., Margana, A., 1995. National Inventory of the Major Lakes and Reservoirs in Indonesia. General Limnology. Helsinki, Expedition Indonau Technical Report. FAO-FINNIDA, pp. 72.
- Lupien, R.L., Russell, J.M., Feibel, C., Beck, C., Castañeda, I., Deino, A., Cohen, A.S., 2018.
  A leaf wax biomarker records of early Pleistocene hydroclimate from West Turkana.
  Kenya. Quat. Sci. Rev. 186, 225–235.
- Meyers, P.A., Teranes, J.L., 2001. Sediment Organic Matter. In: Last, W.M., Smol, J.P. (Eds.), Tracking Environmental Change Using Lake Sediments. Kluwer Academic Publishers. Dordrecht.
- Mohtadi, M., Oppo, D., Steinke, S., Stuut, J.B.W., Pol-Holz, R., Hebbeln, D., Lückge, A., 2011. Glacial to Holocene swings of the Australian-Indonesian monsoon. Nat. Geosci. 4, 540–544.
- Monnier, C., Girardeau, J., Maury, R.C., Cotten, J., 1995. Back-arc basin origin for the East Sulawesi ophiolite (eastern Indonesia). Geology 23, 851–854.
- Morlock, M., Vogel, H., Nigg, V., Ordonez, L., Hasberg, A., Melles, M., Russell, J.M., Bijaksana, S., 2018. Climatic and tectonic controls on source-to-sink processes in the tropical, ultramafic catchment of Lake Towuti. Indonesia. Jour. Paleolim. 61, 279–295.

- Murray, R.W., Miller, D.J., Kryc, K.A., 2000. Analysis of major and trace elements in rocks, sediments, and interstitial waters by inductively coupled plasma—atomic emission spectrometry (ICP-AES). In: Ocean Drilling Program Technical Note, pp. 27 http://www-odp.tamu.edu/publications/tnotes/tn29/INDEX.HTM.
- Niespolo, E.M., Rutte, D., Deino, A.L., Renne, P.R., 2017. Intercalibration and age of the Alder Creek sanidine Ar-40/Ar-39 standard. Quat. Geochronol. 39, 205–213.
- Ninkovich, D., 1979. Distribution, Age, and Chemical Composition of Tephra Layers in Deep-Sea Sediments off Western Indonesia. J. Volcanol. Geotherm. Res. 5, 67–86.
- Penman, H.L., 1948. Natural evaporation from open water, bare soil, and grass. Proceedings of the Royal Society A 193, 120–145.
- Phillips, T.P., Nerem, R.S., Fox-Kemper, B., Famiglietti, J.S., Rajagopalan, B., 2012. The influence of ENSO on global terrestrial water storage using GRACE. Geophys. Res. Lett. 39, L16705 16707 pp.
- Pierrehumbert, R.T., 2000. Climate change and the tropical Pacific: the sleeping dragon wakes. In: Proceedings of the National Academy of Science U.S.A. 97. pp. 1355–1358.
- Poulton, S.W., Canfield, D., 2005. Development of a sequential extraction procedure for irone: implications for iron partitioning in continentally derived particulates. Chem. Geol. 214, 209–211.
- Reeves, J.M., Bostock, H.C., Ayliffe, L.K., Barrows, T.T., De Deckker, P., Devriendt, L.S., Dunbar, G.B., Drysdale, R.N., Fitzsimmons, K.E., Gagan, M.K., Griffiths, M.L., Haberle, S.G., Jansen, J.D., Krause, C., Lewis, S., McGregor, H.V., Mooney, S.D., Moss, P., Nanson, G.C., Purcell, A., van der Kaars, S., 2013. Palaeoenvironmental change in tropical Australasia over the last 30,000 years a synthesis by the OZ-INTIMATE group. Quat. Sci. Rev. 74, 97–114.
- Reimer, P.J., Baillie, M.G.L., Bard, E., Bayliss, A., Beck, J.W., Blackwell, P.G., Bronk Ramsey, C., Buck, C.E., Burr, G.S., Edwards, R.L., Friedrich, M., Grootes, P., Guilderson, T., Hajdas, I., Heaton, T.J., Hogg, A.G., Hughen, K.A., Kaiser, K.F., Kromer, B., McCormac, F.G., Manning, S.W., Reimer, R.W., Richards, D.A., Southon, J.R., Talamo, S., Turney, C.S.M., van der Plicht, J., Weyhenmeyer, C.E., 2009. IntCal09 and Marine09 radiocarbon age calibration curves, 0-50,000 years cal BP. Radiocarbon 51, 1111–1150.
- von Rintelen, T., von Rintelen, K., Glaubrecht, M., Schubart, C., Herder, F., 2012. In: Gower, D.J., Johnson, K.G., Richardson, J.E., Rosen, B.R., Rüber, L., Williams, S.T. (Eds.), Aquatic biodiversity hotspots in Wallacea – the species flocks in the ancient lakes of Sulawesi, Indonesia. Biotic evolution and environmental change in Southeast Asia Cambridge University Press, Cambridge.
- Roy, D., Docker, M.F., Hehanussa, P.E., Heath, D.D., Haffner, G.D., 2004. Genetic and morphological data supporting the hypothesis of adaptive radiation in the endemic fish of Lake Matano. J. Evol. Biol. 17, 1268–1276.
- Ruan, Y., Mohtadi, M., van der Kaars, S., Dupont, L.M., Hebbeln, D., Schefuß, E., 2019. Differential hydroclimatic evolution of East Javanese ecosystems over the past 22.000 years. Ouat. Sci. Rev. 218, 49–60.
- Russell, J.M., Vogel, H., Konecky, B.L., Bijaksana, S., Huang, Y., Melles, M., Wattrus, N., Costa, K., King, J.W., 2014. Glacial forcing of central Indonesian hydrolclimate since 60,000 yr B.P. Proc. Natl. Acad. Sci. 111, 5100–5105.
- Russell, J.M., Bijaksana, S., Vogel, H., Melles, M., Kallmeyer, J., Ariztegui, D., Crowe, S., Fajar, S., Hafidz, A., Haffner, G.D., Hasberg, A., Ivory, S.J., Kelly, C., King, J.W., Kirana, K., Morlock, M., Noren, A., O'Grady, R., Ordonez, L., Stevenson, J., von Rintelen, T., Vuillemin, A., Watkinson, I., Wattrus, N., Wicaksono, S., Wonik, T., Bauer, K., Deino, A., Friese, A., Henny, C., Imran, A.M., Marwoto, R., Ngkoimani, L.O., Nomosatryo, S., Safiuddin, L.O., Simister, R., Tamuntuan, G., 2016. The Towuti Drilling Project: paleoenvironments, biological evolution, and geomicrobiology of a tropical Pacific lake. Sci. Drill. 21, 20–40.
- Sabo, E., Roy, D., Hamilton, P.B., Hehanussa, P.E., McNeely, R., Haffner, G.D., 2008. The plankton community of Lake Matano: factors regulating plankton community composition and relative abundance in an ancient, tropical lake of Indonesia.

- Hydrobiologia 615, 225-235.
- Sarasin, P., Sarasin, F., 1895. Reisebericht aus Celebes. IV. Resie durch Central-Celebes vm Golf von Boni nach den Golf von Tomieni. Verhandlungen der Gerschellschaft für Erdkende 30, 312–352.
- Scholz, C., Rosendhal, B.R., 1988. Low lake stands in Lakes Malawi and Tanganyika, East Africa, delineated with multifold seismic data. Science 240, 1645–1648.
- Sheppard, R.Y., Milliken, R.E., Russell, J.M., Dyar, M.D., Sklute, E.C., Vogel, H., Melles, M., Bijaksana, S., Morlock, M., Hasberg, A., 2019. Characterization of iron in Lake Towuti sediment. Chem. Geol. 512, 11–30.
- Spakman, W., Hall, R., 2010. Surface deformation and slab-mantle interaction during Banda arc subduction rollback. Nat. Geosci. 3, 562–566.
- Stelbrink, B., Stöger, I., Hadiaty, R.K., Schliewen, U.K., Herder, F., 2014. Age estimates for an adaptive lake fish radiation, its mitochondrial introgression, and an unexpected sister group: Sailfin Silversides of the Malili Lakes System in Sulawesi. BMC Evol. Biol. 14, 94.
- Suryamoto, H., Fujimoto, M., Yamakawa, Y., Kosugi, K., Mizuyama, T., 2013. Water balance changes in the tropical rainforest with intensive forest management. Int. J. Sustainable Future for Human Security 2, 56–62.
- Talbot, M.R., Jensen, N.B., Laerdal, T., Filippi, M.L., 2006. Geochemical responses to a major transgression in giant African lakes. J. Paleolimnol. 35, 467–489.
- Tamuntuan, G., Bijaksana, S., King, J.W., Russell, J.M., Fauzi, U., Maryuanani, K., Aufa, N., Safiuddin, L.O., 2015. Variation of magnetic properties in sediments from Lake Towuti, Indonesia, and its paleoclimatic significance. Palaeogeogr. Palaeoclimatol. Palaeoecol. 420, 163–172.
- Tauhid, Y.I., Arifian, J., 2000. Pengamatan Jangka Panjang Kondisi Air Danau Towuti (long-term Observations on the Hydrological Condition of Lake Towuti). Jurnal Sains & Teknologi Modifikasi Cuaca 1, 93–100.
- Vaillant, J.J., Haffner, G.D., Critescu, M.E., 2011. The ancient lakes of Indonesia: toward integrated research on speciation. Integr. Comp. Biol. 51, 634–643.
- Vogel, H., Russell, J.M., Cahyarini, S.Y., Bijaksana, S., Wattrus, N., Rethemeyer, J., Melles, M., 2015. Depositional modes and Lake-level variability at Lake Towuti, Indonesia during the past ~29 kyr BP. Jour. Paleolim. 54, 359–377.
- Vogel, H., Meyer-Jacob, C., Thöle, L., Lippold, J.A., Jaccard, S.L., 2016. Quantification of biogenic silica by means of Fourier transform infrared spectroscopy (FTIRS) in marine sediments. Limnol. Oceanogr. Methods 14, 828–838.
- Vuillemin, A., Friese, A., Alawi, M., Henny, C., Nomosatryo, S., Wagner, D., Crowe, S., Kallmeyer, J., 2016. Geomicrobiological features of ferruginous sediments from Lake Towuti, Indonesia. Front. Microbiol. 7, 1007.
- Vuillemin, A., Wirth, R., Kemnitz, H., Schleicher, A.M., Friese, A., Bauer, K.W., Simister, R., Nomosatryo, S., Ordoñez, L., Ariztegui, D., Henny, C., Crowe, S., Benning, L.G., Kallmeyer, J., Russell, J.M., Bijaksana, S., Vogel, H., 2019. Formation of diagentic siderite in modern ferruginous sediments. Geology 47, 540–544.
- Vuillemin, A., Friese, A., Wirth, R., Schuessler, J.A., Schleicher, A.M., Kemnitz, H., Lucke, A., Bauer, K.W., Nomosatryo, S., Simister, R., Ordoñez, L., Ariztegui, D., Henny, C., Bijaksana, S., Vogel, H., Crowe, S.A., Kallmeyer, J., Russell, J.M., 2020. Vivianite formation in ferruginous sediments from Lake Towuti, Indonesia. Biogeosciences 17, 1955–1973.
- Walpersdorf, A., Vigny, C., Subarya, C., Manurung, P., 1998. Monitoring of the Palu-Koro Fault (Sulawesi) by GPS. Geophys. Res. Lett. 25, 2313–2316.
- Watkinson, I., 2011. Ductile flow in the metamorphic rocks of Central Sulawesi. Geol. Soc. Lond. Spec. Publ. 355, 157–176.
- Wicaksono, S., Russell, J.M., Bijaksana, S., 2015. Compound-specific carbon isotope records of vegetation and hydrologic change in Central Sulawesi, Indonesia, since 53,000 yr bp. Palaeogeogr. Palaeoclimatol. Palaeoecol. 430, 47–56.
- Wilson, T.M., Stewart, C., Sword-Daniels, V., Leonard, G., Johnston, D.M., Cole, J.W., Wardman, J., Wilson, G., Barnard, S., 2011. Volcanic ash impacts on critical infrastructure. Phys. Chem. Earth. https://doi.org/10.1016/l.pce.2011.06.006.